

Title	Optical Anisotropy in Solution-Cast Film of Cellulose Triacetate
Author(s)	Songsurang, Kultida; Miyagawa, Azusa; Abd Manaf, Mohd Edeerozey; Phulkerd, Panitha; Nobukawa, Shogo; Yamaguchi, Masayuki
Citation	Cellulose, 20(1): 83-96
Issue Date	2012-11-02
Type	Journal Article
Text version	author
URL	http://hdl.handle.net/10119/12850
Rights	This is the author-created version of Springer, Kultida Songsurang, Azusa Miyagawa, Mohd Edeerozey Abd Manaf, Panitha Phulkerd, Shogo Nobukawa, Masayuki Yamaguchi, Cellulose, 20(1), 2012, 83-96. The original publication is available at www.springerlink.com , http://dx.doi.org/10.1007/s10570-012-9807-0
Description	

**Optical Anisotropy in Solution-Cast Film
of Cellulose Triacetate**

**Kultida Songsurang, Azusa Miyagawa, Mohd Edeerozey Abd Manaf,
Panitha Phulkerd, Shogo Nobukawa, Masayuki Yamaguchi***

**School of Materials Science
Japan Advanced Institute of Science and Technology**

1-1 Asahidai, Nomi, Ishikawa 923-1292 Japan

***Corresponding Author**

M. Yamaguchi

Phone +81-761-51-1621

Fax +81-761-51-1625

e-mail m_yama@jaist.ac.jp

Abstract

The out-of-plane birefringence and its wavelength dispersion are studied employing solution-cast films of cellulose triacetate (CTA). In solution-cast process, CTA molecules are induced to align in the film plane. Although refractive index is the lowest in the oriented direction for the CTA films stretched more than 110%, refractive index is found to be the lowest in the normal direction for the unstretched cast film. ATR measurements reveal that in-plane alignment of the acetyl group which provides strong polarizability anisotropy is responsible for the phenomenon. Furthermore, the out-of-plane birefringence is found to increase with increasing wavelength, *i.e.*, extraordinary wavelength dispersion, whereas a stretched CTA film shows ordinary wavelength dispersion. The level of the out-of-plane birefringence in cast films depends on the preparation conditions, which is predictable considering the evaporation rate. Moreover, it is demonstrated for the first time that the out-of-plane birefringence and its wavelength dispersion can be modified by addition of a certain plasticizer such as tricresyl phosphate (TCP). During the evaporation, TCP molecules orient in the film plane accompanying the orientation of CTA chains by intermolecular orientation correlation, called nematic interaction. This technique will widen the scope of material design of retardation films because there are numerous liquid compounds having strong polarizability anisotropy.

Keywords: Cellulose Triacetate; Out-of-Plane Birefringence; Solution-Cast

Introduction

With the rapid growth of optical devices these days, there is a continuing trend to develop a potential material for optical films with improved functions and good cost-performance. In particular, cellulose triacetate (CTA), one of the biomass-derived materials, has been studied intensively because of their attractive properties such as high transparency and excellent heat resistant (Edgar et al. 2004; Sata et al. 2004; Yamaguchi 2010; Yamaguchi et al. 2012). At present, CTA films are widely employed in liquid crystal display (LCD) and potentially used for advanced systems such as 3D display and electro-luminescent display in near future. In LCD application, CTA films are used as a polarizer protective film and a retardation (compensation) film. In order to be used in such applications, birefringence control is extremely important. In the case of polarizer protective films, for example, the films have to be free from birefringence, and thus, various methods to erase the birefringence have been proposed recently (Tagaya et al. 2001; Tagaya et al. 2003; Tagaya et al. 2006; Yamaguchi 2010; Yamaguchi et al. 2012). For retardation films, specific retardation, *i.e.*, the product of birefringence and thickness, should be provided. In industries, CTA films are produced by a solution-cast method because melt processing is not applicable due to the severe thermal degradation beyond the melting point (Edgar et al. 2004; Sata et al. 2004; Yamaguchi 2010). Therefore, the information on the molecular orientation and the birefringence of a solution-cast film is significantly important.

For optical anisotropic films, three refractive indices, n_x , n_y and n_z , along three principal axes have to be taken into consideration. The x -axis is the direction showing the maximum refractive index within the film plane in general, the y -axis is the direction perpendicular to the x -axis within the film plane, and the z -axis is the thickness direction and is normal to the x - y plane.

It is well known that a solution-cast method provides films without molecular orientation in the film plane, *i.e.*, $n_x = n_y$. This is the reason why a solution-cast film is preferably employed for a protective film rather than a melt-extruded one. However, the other component of birefringence, namely out-of-plane birefringence, is generally not zero. Therefore, it has to be precisely controlled to provide a high quality display.

In this study, the in-plane birefringence (Δn_{in}) and out-of-plane birefringence (Δn_{th}) are defined by the following equations.

$$\Delta n_{in} = n_x - n_y \quad (1)$$

$$\Delta n_{th} = \frac{n_x + n_y}{2} - n_z \quad (2)$$

Based on the Kuhn and Grün model, the orientation birefringence $\Delta n(\lambda)$ of an oriented polymer is expressed in the following relation (Kuhn and Grün 1942; Treloar 1975; Read 1975; Harding 1986; Marks and Erman 1988).

$$\Delta n(\lambda) = \frac{2\pi}{9} \frac{(\bar{n}(\lambda)^2 + 2)^2}{\bar{n}(\lambda)} N \Delta\alpha(\lambda) \left(\frac{3\langle \cos^2 \theta \rangle - 1}{2} \right) \quad (3)$$

where λ , $\bar{n}(\lambda)$, N , $\Delta\alpha(\lambda)$, and θ are the wavelength of light, the average refractive index, the number of chains in a unit volume, the polarizability anisotropy, and the angle that a segment makes with the stretch axis, respectively. The bracketed term $(3\langle \cos^2 \theta \rangle - 1)/2$ is identically equal to the Hermans orientation function (Hermans and Platzek 1939), which is commonly denoted as F . Therefore, eq. 3 can also be written in the following form for a homogeneous material.

$$\Delta n(\lambda) = \Delta n^0(\lambda)F \quad (4)$$

where $\Delta n^0(\lambda)$ is the intrinsic birefringence.

In the case of a crystalline polymer such as CTA, the contributions from both crystalline and amorphous phases have to be considered even if it has no form birefringence (Stein et al. 1963), as shown in the following equation.

$$\Delta n(\lambda) = \phi_c \Delta n_c^0(\lambda)F_c + (1 - \phi_c) \Delta n_a^0(\lambda)F_a \quad (5)$$

where ϕ_c is the volume fraction of the crystalline phase (degree of crystallinity) and c and a represent crystalline and amorphous regions, respectively.

For solution-cast films, the molecular orientation is caused by the stress induced by solvent removal. The alignment of polymer molecules during a solution-cast process has been investigated by several researchers (Sosnowski and Weber 1972; Croll 1979; Prest and Luca 1979; Prest and Luca 1980; Cohen and Reich 1981; Machell et al. 1990; Greener and Chen 2005; Lei et al. 2001). According to these studies, polymer molecules generally tend to align in a film plane. Consequently, the in-plane refractive indices (n_x and n_y) are higher than the out-of-plane refractive index (n_z) when a material shows positive orientation birefringence. Furthermore, it is known to be difficult to control the out-of-plane birefringence which can affect the performance of the displays.

Sosnowski and Weber (1972) reported that the optical anisotropy in a solution-cast film of polystyrene is given by the result of the stress developed in a coated film during drying process, which makes polymer chains align in the film plane. Prest and Luca (1979) also demonstrated similar results using polystyrene, polycarbonate and poly(2,6-dimethylphenyleneoxide). They showed that the sign of birefringence depends upon the

orientation of the dominating polarizable group relative to the chain backbone. Furthermore, the out-of-plane birefringence was found to be pronounced for a thin film. Prest and Luca (1979, 1980), Cohen and Reich (1981), and Machell et al. (1990) studied the effect of polymer formulations with various casting conditions such as coating thickness, drying temperature and polymer concentration on birefringence values. They found that the out-of-plane birefringence is determined by the competition between the normal stress induced by the drying process and the Brownian motion leading to random conformation by entropic force. Therefore, it is necessary to predict the stress applied by evaporation accurately to evaluate the out-of-plane birefringence. The growth of stress in solution-cast films was studied in detail by several researchers. Croll (1979) developed a simple elastic model to predict the stress, which was later modified by Lei et al. (2001). Greener and Chen (2005) calculated the out-of-plane birefringence by using the model. They found that the out-of-plane birefringence occurs when the solvent concentration is beyond a critical value. At this stage, the compression stress applied in the normal direction to the film plane starts to build up and induces molecular orientation in the film by overcoming the entropic force.

Since the intrinsic birefringence in eqs. 3 and 4 is a function of wavelength, the orientation birefringence is dependent upon the wavelength. Therefore, birefringence control is required in a wide range of visible light. In particular, the extraordinary wavelength dispersion has been desired recently because of the industrial importance for high performance retardation films. The property can provide a specific retardation, *e.g.*, quarter or half of the wavelength, in the whole visible light. However, the wavelength dispersion of most polymers is represented by the following relation called the Sellmeier equation (Kuhn and Grün 1942).

$$\Delta n(\lambda) = A' + \frac{B'}{\lambda^2 - \lambda_{ab}^2} \quad (6)$$

where λ_{ab} is the wavelength of a vibrational absorption peak in ultraviolet region and A' and B' are the Sellmeier coefficients. The equation indicates that the absolute value of birefringence decreases with increasing the wavelength, *i.e.*, ordinary wavelength dispersion.

At present, various techniques are proposed to obtain films showing extraordinary wavelength dispersion. One of the conventional methods is by piling two or more polymer films having different wavelength dispersions, in which the fast axis of one film is set to be parallel to the slow axis of the other films (Yamaguchi et al. 2009a; Mohd Edeerozey et al. 2011a; Yamaguchi et al. 2012). Although this technique is currently employed in industry to fabricate retardation films, it leads to poor cost-performance due to the complicated processing operation and results in a thick display. Therefore, it is more favorable to use a single film with extraordinary wavelength dispersion of birefringence. Blending with another polymer (Uchiyama and Yatabe 2003a; Uchiyama and Yatabe 2003b; Kuboyama et al. 2007) or a low-mass compound (Yamaguchi 2009a; Mohd Edeerozey et al. 2011a), copolymerization with appropriate monomers (Uchiyama and Yatabe 2003c), and addition of nonspherical materials having polarizability anisotropy (Koike et al. 2006) are promising techniques to provide the extraordinary dispersion.

In our preceding paper (Yamaguchi et al., 2009b), it was demonstrated that cellulose acetate propionate (CAP) and cellulose acetate butyrate (CAB) having appropriate substitution of each ester group show extraordinary wavelength dispersion. Moreover, the sign of orientation birefringence of CTA is negative, whereas that of CAP and CAB is positive. It was also shown in the paper that the orientation of main chains is not important to decide the orientation birefringence. Based on these experimental results, it was deduced (but

not proved directly) that the contribution of both acetyl and propionyl/butyryl groups plays an important role in the birefringence, although the contribution of the hydroxyl group was ignored. Because of this complicated origin of the orientation birefringence of cellulose esters, the effect of biaxial mode, such as stretching in one direction with a constant width, has not been clarified yet at the best of our knowledge. Furthermore, the photoelastic birefringence in the glassy state was also investigated and found to be positive even for CTA. The opposite sign of the stress-optical coefficient between rubbery and glassy states for CTA suggests that the origin of the birefringence is completely different between these states, as the same manner with the stress generation. In the case of the rubbery state, the orientation of chain segments decides the birefringence, in which Rouse motion is completely allowed, as assumed in the classical theory of rubber elasticity (Doi and Edwards 1986). On the other hand, the deviation from the location at the lowest potential energy function for atoms in a chain, accompanying bond stretching and/or distortion of bond angle, is responsible for the generation of both stress and birefringence in the glassy state. Therefore, CTA shows positive photoelastic birefringence even after stretching in the glassy state. Moreover, the effect of plasticizer addition is mentioned in this study. Although the species of plasticizers are known to affect the orientation birefringence, the detailed mechanism has not been clarified.

In the following paper (Yamaguchi et al. 2009a), the effect of the hydroxyl group on the orientation birefringence was examined using cellulose diacetate (CDA). It was found that the hydroxyl group provides positive orientation birefringence to a great extent. The result indicates that the hydroxyl group in CAP and CAB plays an important role in the orientation birefringence, although it was not mentioned in the original paper (Yamaguchi et al. 2009b). Moreover, nematic interaction between CTA chains and plasticizer molecules was

indicated during stretching in the rubbery state, which can be applicable to control the wavelength dispersion.

In this study, it is found that the sign of the out-of-plane birefringence in a solution-cast CTA film is opposite to the in-plane orientation birefringence in a hot-stretched one. Moreover, the out-of-plane birefringence in a cast film is found to show extraordinary dispersion. The mechanism of this peculiar phenomenon is discussed in detail. Finally, the effect of nematic interaction in a solution-cast film is also discussed using CTA films containing a specific plasticizer with large polarizability anisotropy, which will be an advanced technique to control the out-of-plane birefringence.

Experimental

Cellulose triacetate (CTA) was obtained from Acros Organic. The degree of substitution is 2.96, and the molecular weight M_w is 3.50×10^5 which was evaluated using a gel permeation chromatograph (Tosoh, HLC-8020) with TSK-GEL[®] GMHXL as polystyrene standard. The plasticizer used in this study was tricresyl phosphate (TCP) produced by Daihachi Chemical Industry. The CTA films were prepared using a solution-cast method. Both CTA and CTA/TCP (95/5 in weight) were dissolved into dichloromethane (CH_2Cl_2) and methanol (CH_3OH) in 9 to 1 weight ratio and stirred for 24 hrs at room temperature before casting. In order to study the effect of solvent, chloroform (CHCl_3) was also employed instead of dichloromethane in the same ratio. The solution containing 4 wt% of CTA was poured into a glass petri dish (80 mm dia x 15 mm H) with a flat bottom at room temperature to allow the solvent to evaporate. The thickness of the films obtained was from 50 to 300 μm , which was controlled by varying the amount of the CTA solution.

During the drying process, evaporation rate was measured by weight loss using an electronic balance (Mettler Toledo, AB204-S). Moreover, the effect of the evaporation rate was investigated by preparing cast films dried with various conditions. A solution dried by exposing directly to the open atmosphere was used as a standard condition for evaporation process. To prepare films with (i) slow and (ii) very slow evaporation conditions, petri dishes containing the solution were covered with an aluminium foil having large and small holes, respectively. The weight loss by evaporation V_e was calculated by the following equation.

$$V_e (\%) = \frac{G_0 - G(t)}{G_0} \times 100 \quad (7)$$

where G_0 is the initial weight of CTA solution; $G(t)$ is the weight of CTA solution after t minutes at room temperature.

The temperature dependence of oscillatory tensile moduli in the solid state was measured from 0 to 250 °C by a dynamic mechanical analyzer (UBM, E-4000) using rectangular specimens with 5 mm in width and 20 mm in length. The frequency and heating rate used were 10 Hz and 2 °C/min, respectively.

Uniaxial oriented films were also prepared by hot-stretching using a tensile machine with a temperature controller (UBM, DVE-3 S1000) at various draw ratios employing rectangular specimens with 10 mm in width. The sample was free from the width direction, *i.e.*, simple extension without width constraint. The initial distance between the clamps was 10 mm, and one of the clamps moved at a stretching rate of 0.5 mm/s. The stretching was performed at the temperature where the tensile storage modulus is 10 MPa at 10 Hz, *i.e.*, 217 °C. After stretching, the drawn sample was quenched immediately by cold air blowing to avoid relaxation of the molecular orientation. Then the sample was removed from the machine to measure the birefringence.

The optical properties of CTA films were measured at room temperature by a polarized optical microscope (Leica, DMLP) and an optical birefringence analyzer (Oji Scientific Instruments, KOBRA-WPR). The retardation in the thickness direction (out-of-plane birefringence) R_{th} was determined by retardation measurements at an oblique incidence angle of 40° as a function of wavelength by changing color filters. The corresponding birefringence was calculated using the film thickness measured by a digital micrometer. Prior to the measurement, the CTA films were placed in a temperature-and-humidity control chamber (Yamato, IG420) at 25°C and 50% RH for one day, because the moisture in the film affects the orientation birefringence (Mohd Edeerozey et al. 2011b). Since a small amount of the water which has strong interaction with acetyl or hydroxyl group cannot be eliminated even under a vacuum condition, this treatment is appropriate to obtain the reproducible data. Although all samples should be fully dried up in a hot vacuum oven prior to this treatment, we avoided it because the thermal history to remove the moisture and solvent will affect the crystalline state of CTA. Furthermore, we confirmed that the exposure to vacuum condition at room temperature for one day does not affect any properties such as dynamic mechanical properties and birefringence, suggesting that the sample does not contain the solvent.

The in-plane retardation (R_{in}) and out-of-plane retardation (R_{th}) are respectively defined as the following relations.

$$R_{in} = \Delta n_{in} \times d = (n_x - n_y) \times d \quad (8)$$

$$R_{th} = \Delta n_{th} \times d = \left(\frac{n_x + n_y}{2} - n_z \right) \times d \quad (9)$$

where d is the film thickness.

The refractive indices in three principal axis, such as n_x , n_y and n_z , are determined by Δn_{in} and Δn_{th} , assuming the average refractive index \bar{n} is a constant irrespective of stretching. The average refractive index \bar{n} was measured by an Abbe refractometer.

Attenuated total reflection (ATR) measurements using an infrared absorption spectrometer (Perkin Elmer, Spectrum 100) were performed to study the molecular orientation in CTA films. The KRS-5 was employed as an ATR crystal.

Thermal analysis was conducted by a differential scanning calorimeter (DSC) (Mettler, DSC820) under a nitrogen atmosphere. The samples were heated from room temperature to 320 °C at a heating rate of 20 °C/min. The amount of samples in an aluminum pan was about 10 mg in weight.

Wide-angle X-ray diffraction (WAXD) measurements were performed at room temperature using a powder X-ray diffractometer (Rigaku, RINT2500) by reflective mode. Samples were mounted directly into the diffractometer. The experiments were carried out using CuK α radiation operating at 40 kV and 30 mA at a scanning rate of 1°/min over 2θ (Bragg angle) range from 5° to 55°.

Results and Discussion

Effect of film thickness

The molecular orientation in the film occurs when the relaxation time of the solution becomes longer than the characteristic time for the biaxial deformation applied by the compressional stress due to the solvent evaporation, which was quantitatively calculated by

Croll (1979). Therefore, the evaporation rate has to be considered to discuss the birefringence in a solution-cast film.

Figure 1 (a) shows the growth curves of the weight loss (in percent) for the CTA solutions to obtain films with various thicknesses. Since all films are prepared using the same petri dish, the thickness is adjusted by the initial volume of the solution. As seen in the figure, the values reach to 96% eventually, suggesting that the solvent is almost fully evaporated at this process. Expectedly, it takes a longer time to prepare a thicker film. This is reasonable because the surface area of the solution is the same irrespective of the film thickness.

In Figure 1 (b), the weight loss (in gram) is plotted against the exposure time. The weight loss is proportional to the exposure time at first, and the slope is constant for all samples. Then, the slope becomes low in the final stage, as CTA retards the solvent evaporation. Considering that the initial slope is the same for all samples, the exposed area of the solution determines the evaporation rate. The result suggests that evaporation occurs homogeneously without creating a solid film on the top of the solution. Moreover, the figures indicate that the stress applied by the reduction of the solution increases with decreasing thickness of the final film because of the rapid drying process. The distribution of molecular orientation, *i.e.*, birefringence, in the thickness direction in the film is confirmed by the polarized optical microscope. Thin films of x - z plane cut out from the cast films by an ultramicrotome are observed under crossed polars by inserting a full wave plate. It is found that a homogeneous birefringence color is detected in the whole area of the specimen, demonstrating that molecular orientation is uniform in the thickness direction. This result indicates that compression deformation takes place uniformly by the solvent evaporation.

[Figure 1]

The wavelength dispersion of the out-of-plane birefringence in cast films is shown in Figure 2. It is found that the solution-cast films of CTA show positive birefringence ($n_z < n_x$, n_y) that increases with increasing wavelength, *i.e.*, extraordinary wavelength dispersion. This is an anomalous phenomenon for a conventional polymer film. The in-plane birefringence is, on the other hand, negligible for all films. Generally, the orientation birefringence of CTA is determined by the contribution of acetyl and hydroxyl groups considering the previous researches at the best of our knowledge (El-Diasty et al. 2007; Yamaguchi et al. 2009a; Yamaguchi et al. 2009b). Since the direction of polarizability anisotropy associated with the acetyl group is perpendicular to the main chain, the refractive index in the oriented direction is the lowest, *i.e.*, negative orientation birefringence. Moreover, it is known that the absolute value of birefringence decreases with increasing the wavelength, *i.e.*, ordinary wavelength dispersion, for CTA, as similar to most conventional polymers (Uchiyama and Yatabe 2003c; Yamaguchi et al. 2009b; Yamaguchi et al. 2010; Yamaguchi et al. 2012). However, the contribution of the hydroxyl group cannot be ignored, which provides positive and ordinary wavelength dispersion (Yamaguchi et al. 2009a).

[Figure 2]

Figure 2 also demonstrates that the birefringence decreases with increasing film thickness, indicating that the refractive index in the in-plane direction decreases with increasing the film thickness. The decrease in the molecular orientation for a thick film is reasonable, because of the slow rate of solvent removal. Since the solvent can be entrapped in a thick film for a long time as shown in Figure 1, the molecules are less oriented in the film plane. Similar results have been reported by another research group, Greener et al. (2005). According to them, a thin film shows a high value of birefringence because the stress builds up faster in the drying process than the stress relaxation.

In order to clarify the effect of film thickness on the birefringence, ATR measurements are performed focusing on the C-O-C stretching vibration in the pyranose ring (1029 cm^{-1}) and C=O stretching vibration in the carbonyl group (1735 cm^{-1}). It should be noted that the same spectra were obtained for both surfaces (air and glass sides), indicating that the skin layer is not well-developed on the free surface (or the contribution of the skin layer on the birefringence can be ignored). As seen in Figure 3, the absorbances of the pyranose ring and the carbonyl group decrease with increasing the film thickness. Considering that the penetration depth of IR beam into the sample is approximately $2.2\text{ }\mu\text{m}$ at 1029 cm^{-1} and $1.2\text{ }\mu\text{m}$ at 1735 cm^{-1} , the film thickness itself does not affect the absorbance. The results indicate that the pyranose ring and the carbonyl group are aligned in the film plane, which is pronounced in a thin, *i.e.*, rapid evaporation film. The in-plane orientation of the carbonyl group will be responsible for the positive out-of-plane birefringence. In the case of a hot-stretched film of CTA, the carbonyl group orients perpendicular to the stretching direction. Consequently, the refractive index in the perpendicular direction is always higher than that in the stretching direction, leading to negative orientation birefringence. On the contrary, the carbonyl group preferably exists in a film plane for a solution-cast film, which is attributed to the in-plane orientation of the pyranose ring. As a result, the refractive index in the film plane is larger than that in the thickness direction, although the backbone chains of CTA are also in the film plane.

[Figure 3]

According to our previous paper (Yamaguchi et al. 2009a), the extraordinary wavelength dispersion for CDA was considered to be attributed to the contributions of the polarizability anisotropy of both hydroxyl and acetyl groups, in which the hydroxyl group in CDA provides positive birefringence with weak wavelength dispersion and the acetyl group

gives negative one with strong wavelength dispersion. Moreover, the magnitude of the birefringence from the hydroxyl group was estimated to be three times as large as that from the acetyl one (Yamaguchi et al. 2009a). In this study, CTA cast films also show extraordinary wavelength dispersion. However, this cannot be explained by the simple summation of both acetyl and hydroxyl groups because of the large amount of the acetyl group. The difference in the wavelength dispersion of refractive indices among three principal directions should be considered to explain the extraordinary dispersion. When n_z shows marked decrease with the wavelength as compared with n_x and n_y , extraordinary wavelength dispersion is expected.

It is also interesting to note that water molecules absorbed in CTA contribute to negative orientation birefringence slightly, at which the magnitude of the birefringence change is almost independent of the wavelength (Mohd Edeerozey et al. 2011b).

In the case of CTA, the crystallization state has to be considered, because it is well known that CTA is a crystalline polymer (Watanabe et al. 1968; Takahashi et al. 1979; Cao et al. 2000; Sata 2004; Cerqueira et al. 2006). Irrespective of the crystallinity, CTA films always exhibit high level of transparency. This is attributed to the reduced light scattering originated from the polarizability difference of crystalline aggregates, because the correlation distance is shorter than the wavelength of visible light as discussed previously (Norris and Stein 1958; Tenma and Yamaguchi 2004). The heat of fusion of the perfect CTA crystal has been discussed for a long time after the pioneering work by Takahashi et al. (1979). The value was recently reported to be 58.8 J/g by Cerqueira et al. (2006).

As shown in Table 1, it is found that the degree of crystallization is almost constant irrespective of the film thickness. The degree of the crystallization is calculated to be 17 – 23 wt% based on the literature data (Cerqueira et al. 2006). Furthermore, WAXD measurements

are also carried out and shown in Figure 4. The top pattern in the figure will be discussed later. It is found from the bottom pattern in Figure 4 that a broad peak is detected around 7-8 degree with amorphous background, which is a similar diffraction pattern to that reported by Cao et al. (2000). The result indicates that the orientation birefringence has to be discussed using eq. 5. However, we avoid the discussion on the contribution of crystalline phase, at least for cast films, because it is difficult to obtain the information on the intrinsic birefringence as well as the orientation function of both amorphous and crystalline phases separately.

[Table 1][Figure 4]

It can be concluded from Figures 1-3, the achievable anisotropy is found to be a function of the evaporation rate. Therefore, further study is performed focusing the effect of evaporation rate.

Effect of evaporation rate

The evaporation rate is controlled by covering the petri dishes with an aluminium foil. The growth curves of the weight loss are shown in Figure 5. In the figure, the “standard” represents the cast film obtained by drying uncovered petri dishes, the same drying method to the samples in Figure 1. The “slow” and “very slow” denote the cast films obtained with an aluminium foil having large and small holes, respectively. The thickness of all films is approximately 100 μm . As seen in the figure, the evaporation rate can be controlled by this technique. The initial slope of the standard is three times larger than that of the very slow.

[Figure 5]

The wavelength dispersion of the out-of-plane birefringence of the samples is shown in Figure 6. All films show positive birefringence with extraordinary wavelength dispersion irrespective of the evaporation rate. However, the magnitude of the birefringence increases with increasing the evaporation rate. Therefore, a similar situation with a thick film occurs for the film evaporated slowly. The decrease in the birefringence for a film obtained by the prolonged evaporation process suggests that stress, *i.e.*, molecular orientation, is relaxed. It is reasonable because the polymer chains are able to move randomly during the cast process.

[Figure 6]

The effect of the evaporation rate on the crystallization of CTA is also studied by DSC. As shown in Table 1, however, the heat of fusion, and thus, the degree of crystallization is not changed at this experimental condition.

Effect of solvent type

The species of solvents affects the evaporation rate and thus the out-of-plane birefringence, as shown in Figures 7 and 8, respectively. As seen in Figure 7, the evaporation rate of the mixed solvent of CH_2Cl_2 and CH_3OH is faster than that of CHCl_3 and CH_3OH , because the vapor pressure of CH_2Cl_2 is higher than that of CHCl_3 at room temperature. Moreover, it is identified that the whole curve of the $\text{CHCl}_3/\text{CH}_3\text{OH}$ solution is almost the same as that of the $\text{CH}_2\text{Cl}_2/\text{CH}_3\text{OH}$ solution with an aluminium foil having small holes (“slow” in Figure 5). The result demonstrates that the retardant effect of the evaporation by CTA is almost the same for both solvents. This would be attributed to similar molecular interaction with CTA for both solvents.

[Figure 7] [Figure 8]

Because of the difference in the evaporation rate, the relaxation of molecular orientation of CTA is pronounced for the $\text{CHCl}_3/\text{CH}_3\text{OH}$ solution as long as the evaporation condition is the same. Therefore, the CTA film prepared by $\text{CH}_2\text{Cl}_2/\text{CH}_3\text{OH}$ shows higher out-of-plane birefringence than the film by $\text{CHCl}_3/\text{CH}_3\text{OH}$, as seen in Figure 8.

The out-of-plane birefringence at 588 nm is plotted against the evaporation rate as shown in Figure 9. The evaporation rate here refers to the initial slope of the weight loss versus time. As seen in the figure, the birefringences of the films obtained from the $\text{CHCl}_3/\text{CH}_3\text{OH}$ and $\text{CH}_2\text{Cl}_2/\text{CH}_3\text{OH}$ solutions fall on the same line. The result demonstrates that the out-of-plane birefringence is independent of the species of solvents, but depends on the evaporation rate.

[Figure 9]

Effect of plasticizer

Recently, it has been clarified that addition of specific plasticizers is able to control the orientation birefringence of a stretched film. In particular, it was found that orientation birefringence is enhanced by TCP for cellulose esters (Mohd Edeerozey et al. 2011a). The phenomenon is explained by nematic interaction, *i.e.*, intermolecular orientation correlation (Doi and Watanabe 1991; Watanabe et al. 1991). Although TCP is a low mass compound in the liquid state, the molecules are forced to orient in the same direction with the polymer chains. Considering that the nematic interaction occurs when the size of a low mass compound is comparable with the segmental size of a matrix polymer (Urakawa et al. 2006; Nobukawa et al. 2010; Nobukawa et al. 2011), TCP has an appropriate size for CTA. To the

best of our knowledge, however, the nematic interaction in solution-cast films has not been studied yet.

Figure 10 shows the out-of-plane birefringence of a CTA film containing 5 wt% of TCP with the data of pure CTA. As seen in the figure, addition of TCP greatly enhances the out-of-plane birefringence of CTA. Since the evaporation rate is not affected by the addition of TCP (but not presented here), the enhancement is attained by the orientation of TCP molecules in the film plane accompanied with CTA chains. Also in this experiment, the degree of crystallization remains unchanged as shown in Table 1.

[Figure 10]

In order to confirm the contribution of TCP to the birefringence, the CTA/TCP film is immersed in methanol for 24 hrs to remove TCP. Then, the out-of-plane birefringence is measured again after drying at room temperature under a vacuum condition. Prior to the measurement, it is ensured that the methanol immersion does not affect the birefringence of pure CTA. The removal of TCP is confirmed by FT-IR spectra, and the sample is kept in the temperature-and-humidity controller for 24 hrs before being measured for birefringence. The FT-IR spectrum for CTA/TCP shows a strong absorption peak around 780 cm^{-1} , which is not detected in CTA but appears in TCP spectrum. This peak is attributed to the vibration of C-H bond in meta-disubstituted benzene of TCP (Mohd Edeerozey et al. 2011a). Therefore, the lack of this peak suggests that TCP has been completely removed out. After methanol immersion, the birefringence of CTA/TCP decreases approaching to that of pure CTA, as illustrated in Figure 11. The result demonstrates that TCP molecules oriented by nematic interaction enhance the out-of-plane birefringence. In other words, the out-of-plane birefringence can be controlled by not only evaporation rate but also additives.

As mentioned in the introduction, the competition of molecular motion and deformation applied by the solvent evaporation determines the molecular orientation in a solution-cast film. In other words, CTA chains orient in the film plane by applied uniaxial compression deformation due to the solvent evaporation. At the same time, TCP molecules orient cooperatively with the CTA chains. Therefore, the orientation relaxation of TCP molecules will be affected strongly by the existence of a solvent, although the relaxation time is reduced for both CTA and TCP. The experimental results indicate that the nematic interaction, *i.e.*, orientation of TCP molecules, occurs only at the final stage of evaporation. Therefore, a solvent that retards the evaporation rate at the final stage to obtain smooth surface will have a strong influence on the orientation of additives.

[Figure 11]

Effect of hot-stretching

The hot-stretching is performed at 217 °C, at which the tensile storage modulus at 10 Hz was 10 MPa, *i.e.*, rubbery state. The stress-strain curve is shown in Figure 12, which is a typical one for a viscoelastic body in the rubbery region.

[Figure 12]

The refractive indices at 588 nm along three principle axes for films with various draw ratios are illustrated in Figure 13. In this experiment, the hot-stretching was performed in the x direction.

As mentioned, the unstretched film is randomly oriented in the film plane, *i.e.*, $n_x = n_y$, but the principle refractive index in the thickness direction n_z is lower than n_x and n_y ,

which results in the positive out-of-plane birefringence. On the contrary, a hot-drawn film shows negative in-plane birefringence.

[Figure 13]

The wavelength dispersion of in-plane and out-of-plane birefringences for the stretched films is shown in Figure 14. As seen in the figure, the order in the refractive indices changes with the draw ratio. When the draw ratio is around 1.035, n_z is almost the same as $(n_x+n_y)/2$ at 588 nm. Beyond this draw ratio, the out-of-birefringence of the unstretched sample shows extraordinary wavelength dispersion, whereas in-plane and out-of-plane birefringences for the stretched films exhibit ordinary wavelength dispersion. Moreover, the out-of-birefringence of the stretched films is almost independent of the applied strain level, when the draw ratio is larger than 1.1.

The negative in-plane birefringence in CTA suggests that the direction of the polarizability anisotropy associated with the acetyl group is perpendicular to the main chain. This result corresponds with the previous reports (El-Diasty et al. 2007; Yamaguchi et al. 2009a; Mohd Edeerozey et al. 2011ab).

Because the hot-stretching is carried out beyond the glass transition temperature, the degree of crystallinity has to be considered more seriously. The top pattern in Figure 4 shows the WAXD profile of a stretched film at a draw ratio of 1.5. As seen in the figure, several distinct peaks are clearly detected, which are attributed to the thermal history beyond the glass transition temperature with the flow induced crystallization during stretching. Therefore, the contribution of crystalline phase cannot be ignored especially after hot-stretching. It was found that the extraordinary wavelength dispersion of CAP becomes pronounced with increasing the draw ratio (Yamaguchi et al. 2009a). The result indicates that

the acetyl group plays a more important role in the total birefringence with increasing the draw ratio. A similar situation is expected also for CTA, because the acetyl group is in the crystalline structure with the strong polarizability anisotropy in the direction perpendicular to the chain axis (Sikorski et al. 2004). In other words, the wavelength dispersion and the magnitude of birefringence for CTA, including solution-cast films, can be modified by controlling the crystalline state.

[Figure 14]

Conclusion

The orientation birefringence of CTA films produced by a solution-cast method is studied. Prior to stretching, the CTA film shows positive out-of-plane birefringence with extraordinary wavelength dispersion, whereas the stretched film shows negative in-plane birefringence. The positive birefringence is attributed to the in-plane orientation of the acetyl group in CTA, which is confirmed by ATR. Furthermore, it is found that a thin film shows marked birefringence, which is originated from the molecular orientation in the film plane due to the stress applied by the solvent evaporation. Similarly, prompt evaporation enhances the birefringence irrespective of the species of solvents. Moreover, the out-of-plane birefringence of CTA is found to increase with the addition of TCP. This is attributed to the molecular orientation of TCP by the nematic interaction, *i.e.*, intermolecular orientation correlation, between CTA and TCP.

References

- Cao S, Shi Y, Chen G (2000) Influence of acetylation degree of cellulose acetate on prevaporation properties for MeOH/MTBE mixture. *J Membrane Sci* 165(1):89-97.
- Cerqueira DA, Filho GR, Assuncao RM (2006) A new value for the heat of fusion of a perfect crystal of cellulose acetate. *Polym Bull* 56(4-5):475-484.
- Cohen Y, Reich S (1981) Ordering phenomena in thin polystyrene films, *J Polym Sci Polym Phys Ed* 19(4):599-608.
- Croll SG (1979) The origin of residual internal stress in solvent-cast thermoplastic coatings. *J Appl Polym Sci* 23(3):847-858.
- Doi M, Edwards SF (1986) *The theory of polymer dynamics*. Oxford Science Publications: Oxford.
- Doi M, Watanabe H (1991) Effect of nematic interaction on the Rouse dynamics. *Macromolecules* 24(3):740-744.
- Edgar KJ, Buchanan CM, Debenham JS, Rundquist PA, Seiler BD, Shelton MC, Tindall D (2001) Advances in cellulose ester performance and application. *Prog Polym Sci* 26(9):1605-1688
- El-Diasty F, Soliman MA, Elgendy AFT, Ashour A (2007) Birefringence dispersion in uniaxial material irradiated by gamma rays: cellulose triacetate films. *J Opt A Pure Appl Opt* 9(3):247-252.
- Greener J, Chen J. (2005) Optical properties of solvent-cast polarizer films for liquid crystal displays, *IDMC Taipei, Taiwan*.
- Greener J, Lei H, Elman J, Chen J (2005) Optical properties of solvent-cast polarizer films for liquid-crystal displays: A viscoelastic modeling framework. *J SID* 13(10):835-839.
- Harding GF (1986) *Optical properties of polymers*, Meeten GH, Ed.; Applied and Science: London, Chap. 2.
- Hermans PH, Platzek P (1939) Beitrage zur kenntnis des deformationsmechanismus und der feinstruktur der hydratzellulose X. die Kratky'sche kette als rechenmodell für deformationsmechanismus der hydratzellulosegele. *Kolloid-Z* 88(1):68-72.
- Koike Y, Yamazaki K, Ohkita H, Tagaya A (2006) Zero-birefringence optical polymer by birefringent crystal and analysis of the compensation mechanism. *Macromol Symp* 235(1):64-70.
- Kuboyama K, Kuroda T, Ougizawa T (2007) Control of wavelength dispersion of birefringence by miscible polymer blends. *Macromol Symp* 249-250(1):641-646.

- 553 Kuhn W, Grün F (1942) Beziehungen zwischen elastischen konstanten und
554 dehnungsdoppelbrechung hochelastischer stoffe. *Kolloid-Z* 101(3), 248-271.
- 555 Lei H, Payne A, McCormick AV, Francis LF, Gerberich WW, Scriven LE (2001) Stress
556 development in drying coatings. *J Appl Polym Sci* 81(4):1000-1013.
- 557 Machell JS, Greener J, Contestable BA (1990) Optical properties of solvent cast polymer
558 films. *Macromolecules* 23(1):186-194.
- 559 Marks JE, Erman B (1988) Rubberlike elasticity A molecular primer, Wiley: New York.
- 560 Mohd Edeerozey AM, Tsuji M, Shiroyama Y, Yamaguchi M (2011a) Wavelength dispersion
561 of orientation birefringence for cellulose esters containing tricresyl phosphate.
562 *Macromolecules* 44(10):3942-3949.
- 563 Mohd Edeerozey AM, Tsuji M, Nobukawa S, Yamaguchi M (2011b) Effect of moisture on
564 the orientation birefringence of cellulose esters. *Polymers* 3(2):955-966.
- 565 Nobukawa S, Urakawa O, Shikata T, Inoue T (2010) Evaluation of nematic interaction
566 parameter between polymer segments and low-mass molecules in the mixture.
567 *Macromolecules* 43(14):6099-6105.
- 568 Nobukawa S, Urakawa O, Shikata T, Inoue T (2011) Cooperative dynamics in polystyrene
569 and low-mass molecule mixtures. *Macromolecules* 44(20):8324-8332.
- 570 Norris FH, Stein RS (1958) The scattering of light from thin polymer films IV. Scattering
571 from oriented polymers. *J Polym Sci* 27(1):87-114.
- 572 Prest WM, Luca DJ (1979) The origin of the optical anisotropy of solvent cast polymeric
573 films. *J Appl Phys* 50(10):6067-6072.
- 574 Prest WM, Luca DJ (1981) The alignment of polymers during the solvent - coating process.
575 *J Appl Phys* 51(10):5170-5175.
- 576 Read BE (1975) Structure and properties of oriented polymers, Ward IM. Ed.; Applied
577 Science Publishers: London, Chap. 4.
- 578 Sata H, Murayama M, Shimamoto S (2004) Properties and applications of cellulose triacetate
579 film. *Macromol Symp* 208(1):323-333.
- 580 Sikorski P, Wada M, Heux L, Shintani H, Stokke B (2004) Crystal structure of cellulose
581 triacetate I 37(12):4547-4553.
- 582 Sosnowski TP, Weber HP (1972) Thin birefringent polymer films for integrated optics. *Appl*
583 *Phys Lett* 21(7):310-312.
- 584 Stein RS, Onogi S, Sasaguri K, Keedy DA (1963) Dynamic birefringence of high polymers II.
585 *J Appl Phys* 34(1):80-89.

- 586 Tagaya A, Iwata S, Kawanami E, Tsukahara H, Koike Y (2001) Anisotropic molecule dopant
587 method for synthesizing a zero-birefringence polymer. *Jpn J Appl Phys* 40(10):6117-
588 6123.
- 589 Tagaya A, Ohkita H, Mukoh M, Sakaguchi R, Koike Y (2003) Compensation of the
590 birefringence of a polymer by a birefringent crystal. *Science* 301:812-814.
- 591 Tagaya A, Ohkita H, Harada T, Ishibashi K, Koike Y (2006) Zero-birefringence optical
592 polymers. *Macromolecules* 39(8):3019-3023.
- 593 Takahashi A, Kawaharada T, Kato T (1979) Melting temperature of thermally reversible gel.
594 V. heat of fusion of cellulose triacetate and the melting of cellulose diacetate-benzyl
595 alcohol gel. *Polym J* 11(8):671-675.
- 596 Tenma M, Yamaguchi M (2007) Structure and properties of injection-molded polypropylene
597 with sorbitol-based clarifier. *Polym Eng Sci* 47(9):1441-1446.
- 598 Treloar LRG (1958) *The physics of rubber elasticity*, Clarendon Press: Oxford.
- 599 Uchiyama A, Yatabe T (2003a) Analysis of extraordinary birefringence dispersion of
600 uniaxially oriented poly(2,6-dimethyl 1,4-phenylene oxide)/atactic polystyrene blend
601 films. *Jpn J Appl Phys* 42(6):3503-3507.
- 602 Uchiyama A, Yatabe T (2003b) Control of birefringence dispersion of uniaxially oriented
603 poly(2,6-dimethyl 1,4-phenylene oxide)/atactic polystyrene blend films by changing the
604 stretching parameters. *Jpn J Appl Phys* 42(11):5665-5669.
- 605 Uchiyama A, Yatabe T (2003c) Control of wavelength dispersion of birefringence for
606 oriented copolycarbonate films containing positive and negative birefringent units. *Jpn J*
607 *Appl Phys* 42(11):6941-6945.
- 608 Urakawa O, Ohta E, Hori H, Adachi K (2006) Effect of molecular size on cooperative
609 dynamics of low mass compounds in polystyrene. *J Polym Sci Polym Phys Ed*
610 44(6):967-974.
- 611 Yamaguchi M, Okada K, Mohd Edeerozey AM, Shiroyama Y, Iwasaki T, Okamoto K
612 (2009a) Extraordinary wavelength dispersion of orientation birefringence for cellulose
613 esters. *Macromolecules* 42(22):9034-9040.
- 614 Yamaguchi M, Iwasaki T, Okada K, Okamoto K (2009b) Control of optical anisotropy of
615 cellulose esters and their blends with plasticizer. *Acta Materialia* 57(3):823-829.
- 616 Yamaguchi M, Lee S, Mohd Edeerozey AM, Tsuji M, Yokohara T (2010) Modification of
617 orientation birefringence of cellulose ester by addition of poly(lactic acid). *Eur Polym J*
618 46(12):2269-2274.

- 619 Yamaguchi M (2010) Optical properties of cellulose esters and their blends, in Cellulose:
620 structure and properties, derivatives, and industrial uses, Eds., Lejeune A, Deprez T.
621 Chap. 17, Nova Science Publishers, New York.
- 622 Yamaguchi M, Mohd Edeerozey AM, Songsurang K, Nobukawa S (2012) Material design of
623 retardation films with extraordinary wavelength dispersion of orientation birefringence -
624 A review. Cellulose, 19 (3):601-613.
- 625 Watanabe H, Kotaka T, Tirrell M (1991) Effect of orientation coupling due to nematic
626 interaction on relaxation of Rouse chains. Macromolecules, 24(1):201-208.
- 627 Watanabe S, Takai M, Hayashi J (1968) An X-ray study of cellulose triacetate. J Polym Sci
628 Part-C Polym Symp, 23(2):825-835.
- 629

Table Caption

Table 1 Thermal Properties of Solution-Cast Films Obtained by Various Conditions

Figure Captions

Figure 1 (a) Growth curves of the weight loss (%) for CTA solutions to obtain films with various thicknesses; 50 μm (circles), 100 μm (diamonds), 200 μm (triangles) and 300 μm (squares).

Figure 1 (b) Growth curves of the weight loss (g) for CTA solutions to obtain films with various thicknesses; 50 μm (circles), 100 μm (diamonds), 200 μm (triangles) and 300 μm (squares).

Figure 2 Wavelength dispersion of out-of-plane birefringence for cast films with various thicknesses; 50 μm (circles), 100 μm (diamonds), 200 μm (triangles) and 300 μm (squares).

Figure 3 Relation between film thickness and absorbances of pyranose ring (A_{1029}) (circles) and carbonyl group (A_{1735}) (diamonds) for cast films obtained from $\text{CH}_2\text{Cl}_2/\text{CH}_3\text{OH}$ at the standard condition.

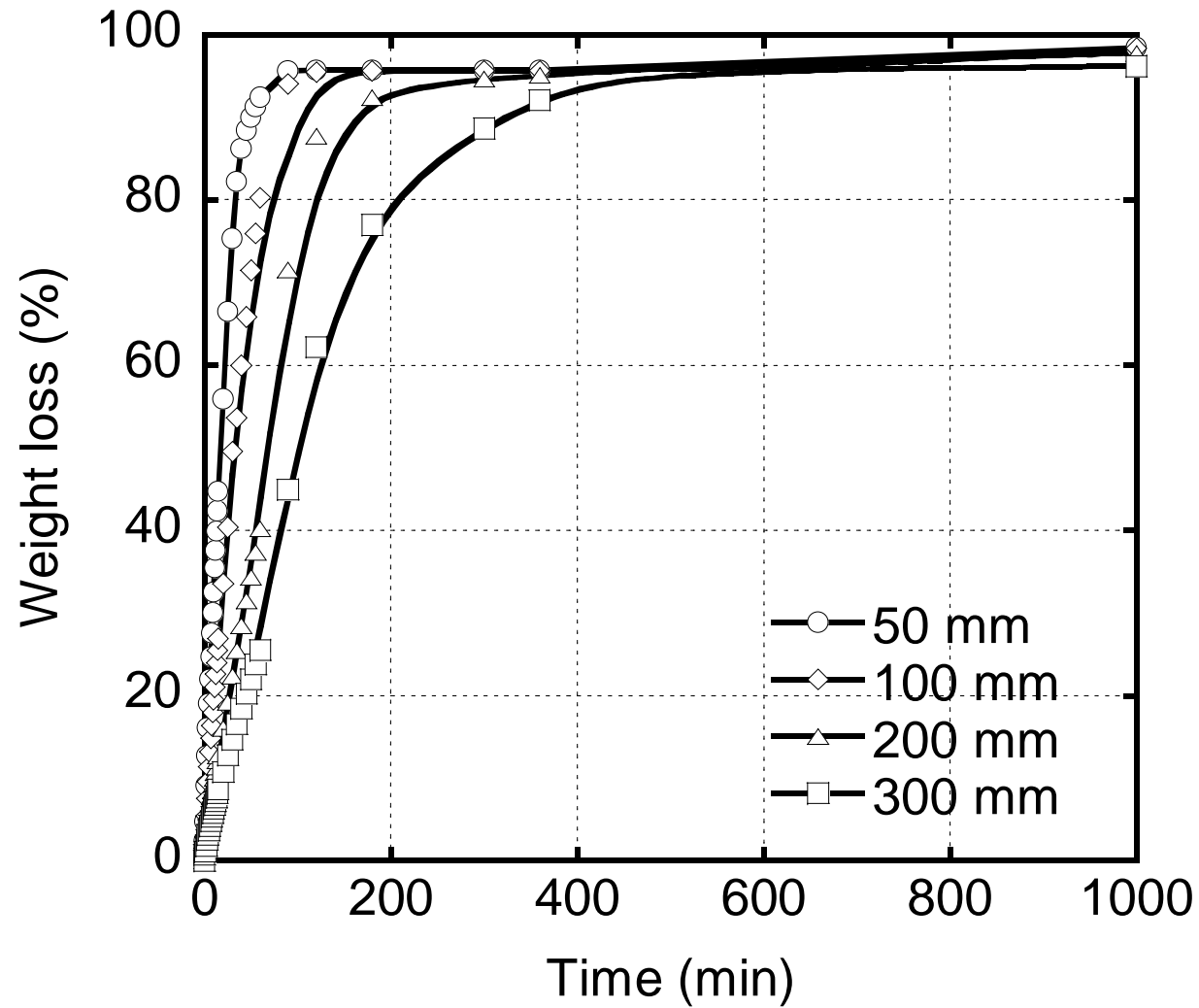
Figure 4 Wide-angle X-ray diffraction patterns for (bottom) a cast film with a thickness of 100 μm obtained from $\text{CH}_2\text{Cl}_2/\text{CH}_3\text{OH}$ at a standard condition, and (top) a film stretched at a draw ratio of 1.5.

Figure 5 Growth curves of the weight loss (%) for CTA solutions at various evaporation rates; standard (circles), slow (diamonds) and very slow (triangles).

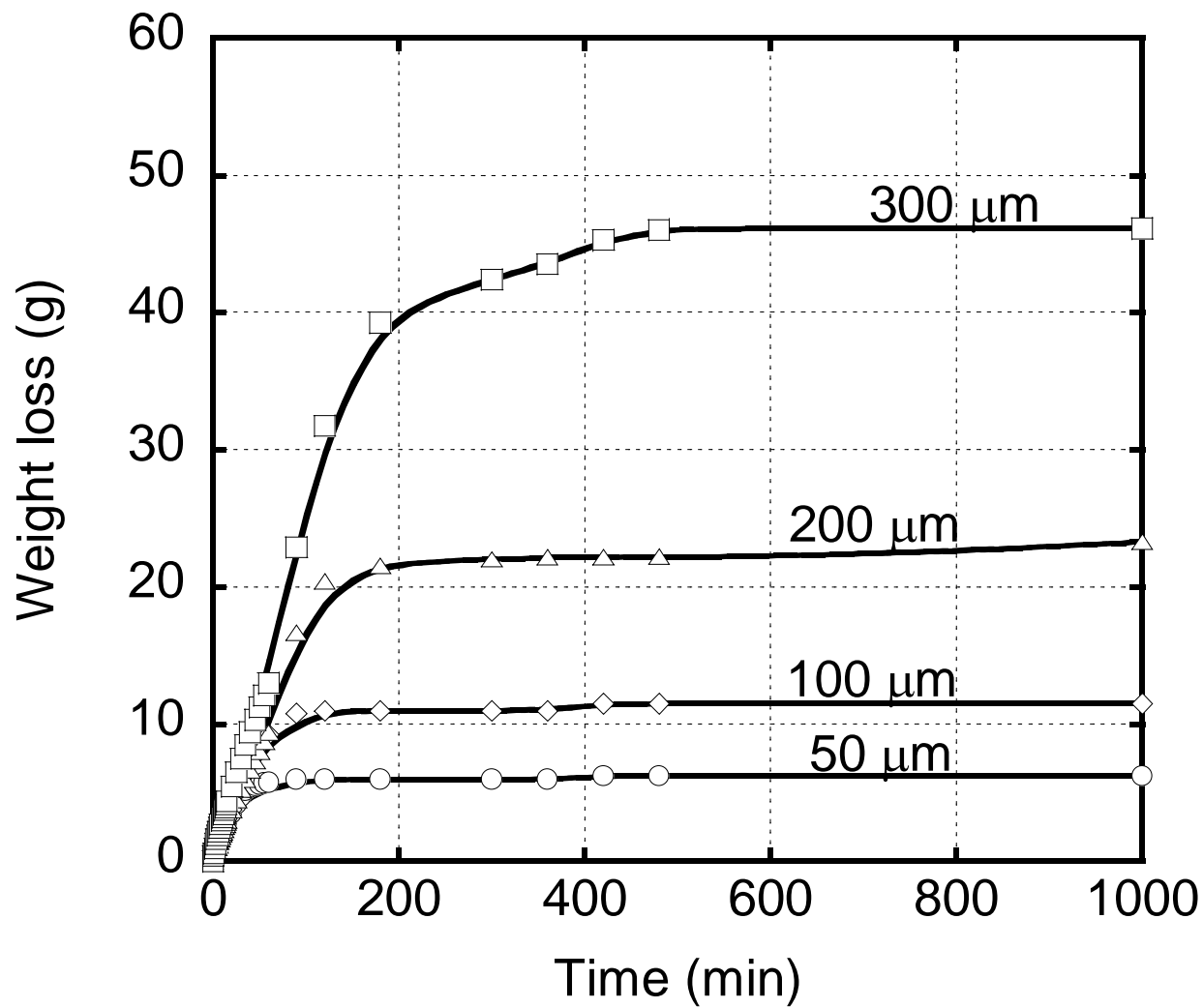
- 651 Figure 6 Wavelength dispersion of out-of-plane birefringence for films obtained at
652 various evaporation rates; standard (circles), slow (diamonds) and very slow
653 (triangles).
- 654 Figure 7 Growth curves of the weight loss (%) for CTA solutions using $\text{CH}_2\text{Cl}_2/\text{CH}_3\text{OH}$
655 (circles) and $\text{CHCl}_3/\text{CH}_3\text{OH}$ (diamonds) as solvents.
- 656 Figure 8 Wavelength dispersion of out-of-plane birefringence for the cast films obtained
657 from $\text{CH}_2\text{Cl}_2/\text{CH}_3\text{OH}$ (circles) and $\text{CHCl}_3/\text{CH}_3\text{OH}$ (diamonds) at the standard
658 condition. The thickness of the films was 100 μm .
- 659 Figure 9 Out-of-plane birefringence at 588 nm for the cast films plotted against the initial
660 slope of the weight loss (g); $\text{CH}_2\text{Cl}_2/\text{CH}_3\text{OH}$ (standard) (circle),
661 $\text{CH}_2\text{Cl}_2/\text{CH}_3\text{OH}$ (slow) (diamond), $\text{CH}_2\text{Cl}_2/\text{CH}_3\text{OH}$ (very slow) (triangle) and
662 $\text{CHCl}_3/\text{CH}_3\text{OH}$ (standard) (square).
- 663 Figure 10 Wavelength dispersion of out-of-plane birefringence for CTA (circles) and
664 CTA/TCP (diamonds). The cast films with a thickness of 100 μm were
665 prepared by $\text{CH}_2\text{Cl}_2/\text{CH}_3\text{OH}$ at the standard condition.
- 666 Figure 11 Wavelength dispersion of out-of-plane birefringence for CTA/TCP before
667 (closed diamonds) and after immersion in methanol (open diamonds). The
668 original cast film with a thickness of 100 μm was prepared by $\text{CH}_2\text{Cl}_2/\text{CH}_3\text{OH}$
669 at the standard condition.
- 670 Figure 12 Stress (σ) – strain (ε) curve at 217 $^\circ\text{C}$ for CTA. The cast film with a thickness of
671 100 μm was prepared by $\text{CH}_2\text{Cl}_2/\text{CH}_3\text{OH}$ at the standard condition.

672 Figure 13 Refractive indices along three principle axes; n_x (circles), n_y (triangles) and n_z
673 (diamonds) for CTA films stretched at various draw ratios. The original cast
674 films with a thickness of 100 μm were prepared by $\text{CH}_2\text{Cl}_2/\text{CH}_3\text{OH}$ at the
675 standard condition.

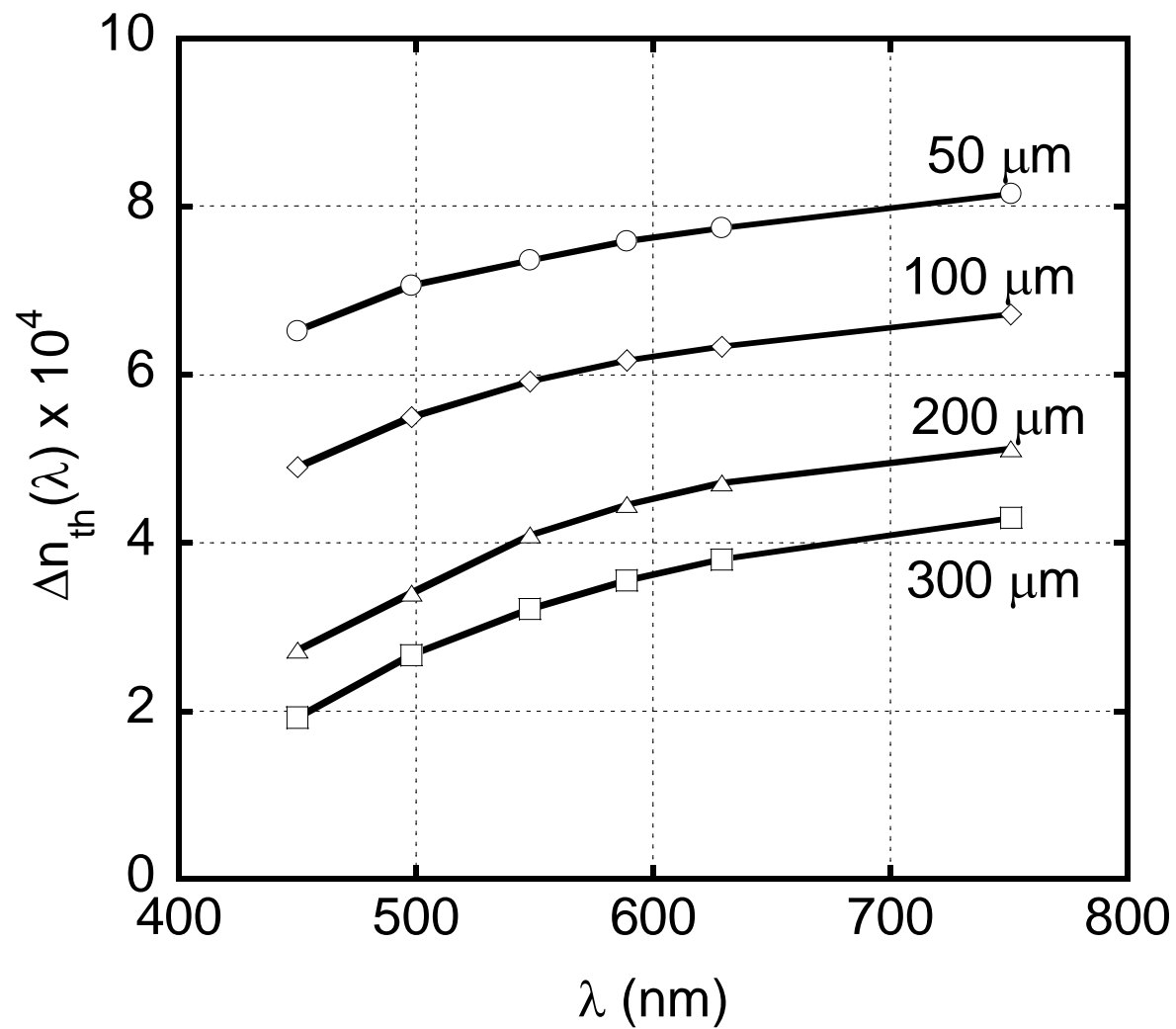
676 Figure 14 Wavelength dispersion of (a) in-plane birefringence and (b) out-of-plane
677 birefringence for a cast film (circles) and stretched films with draw ratios of 1.1
678 (diamonds), 1.3 (triangles), and 1.5 (squares). The cast films with a thickness of
679 100 μm were prepared by $\text{CH}_2\text{Cl}_2/\text{CH}_3\text{OH}$ at the standard condition.



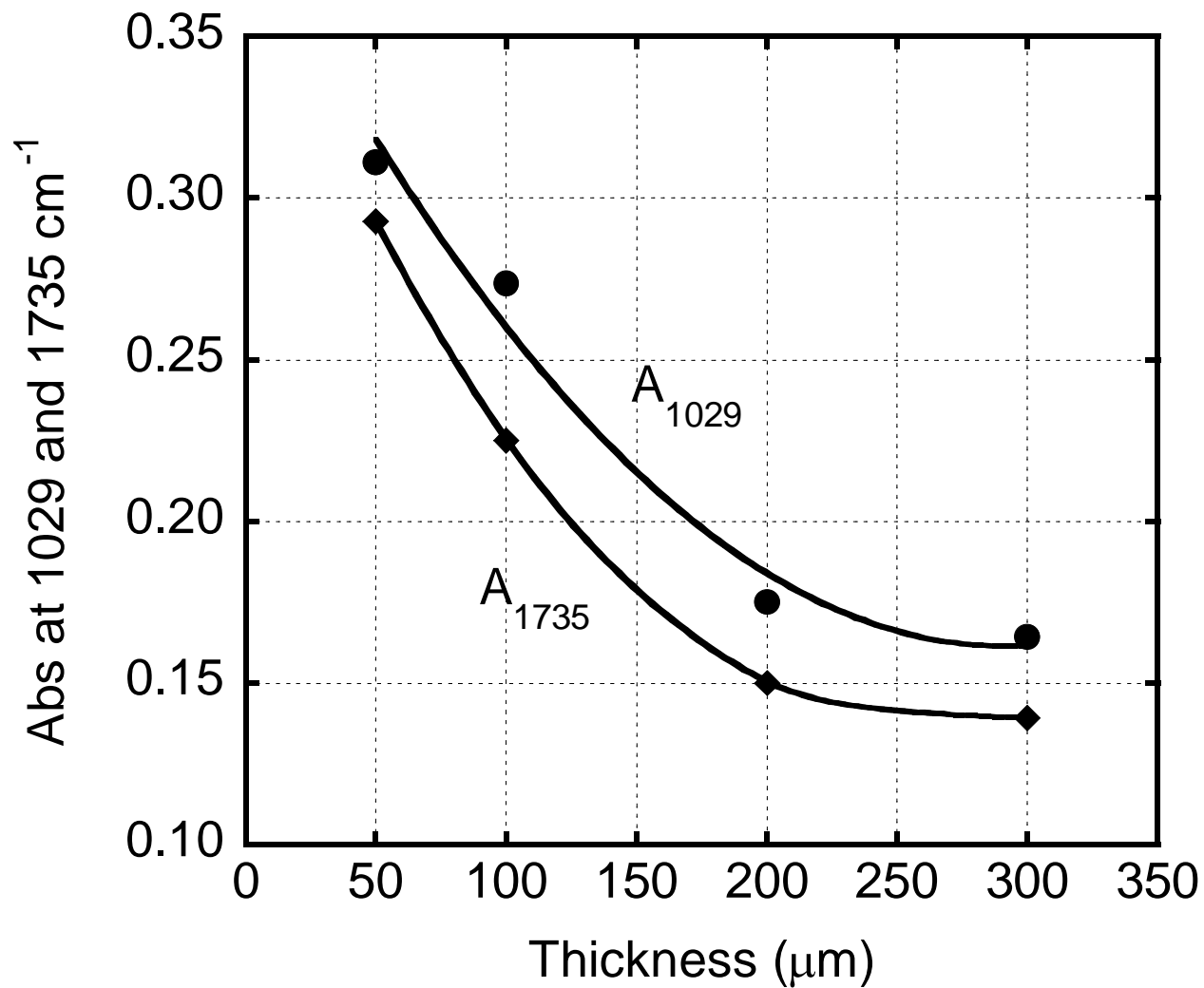
Songsurang et al., Figure 1 (a)



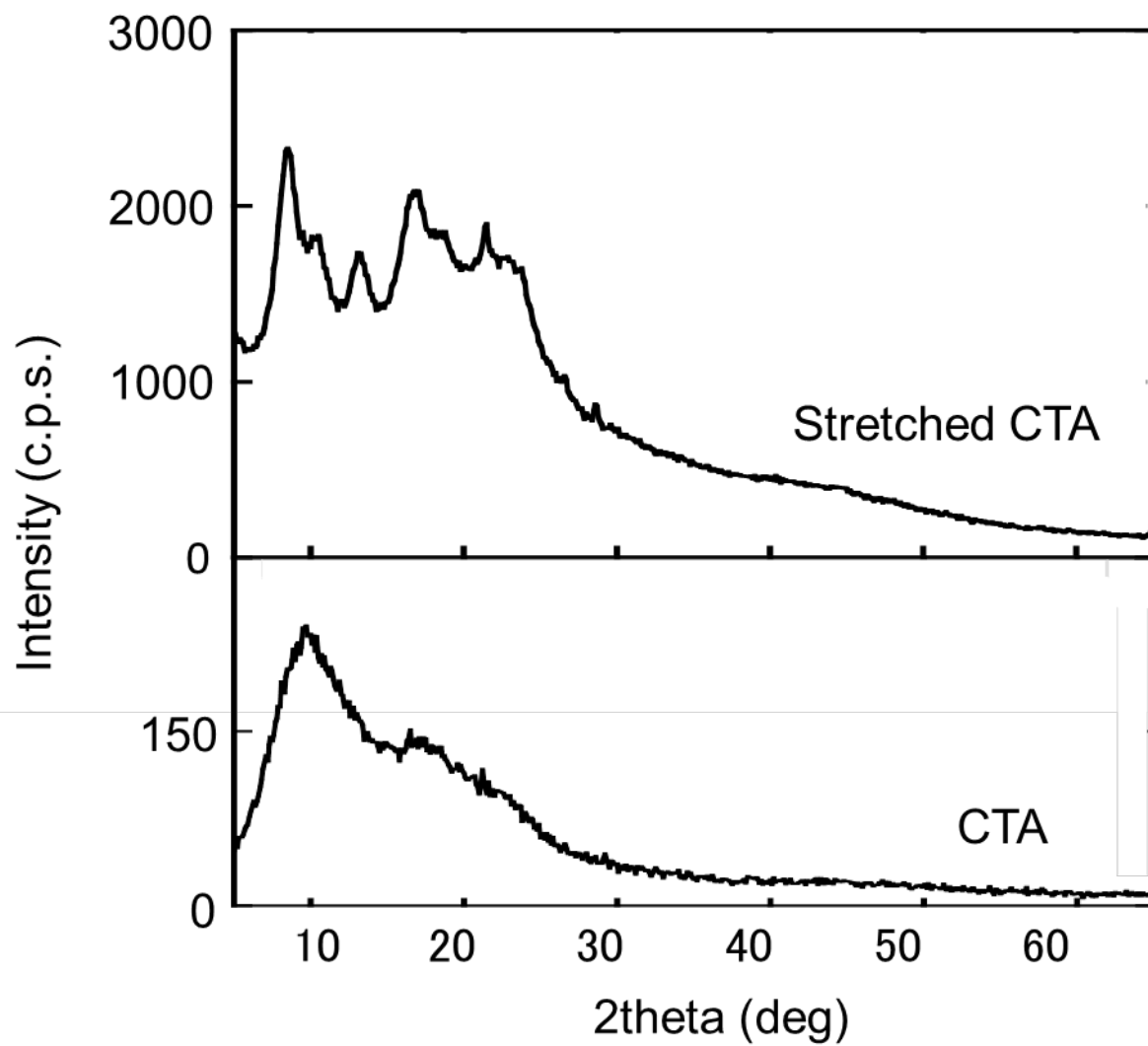
Songsurang et al., Figure 1 (b)



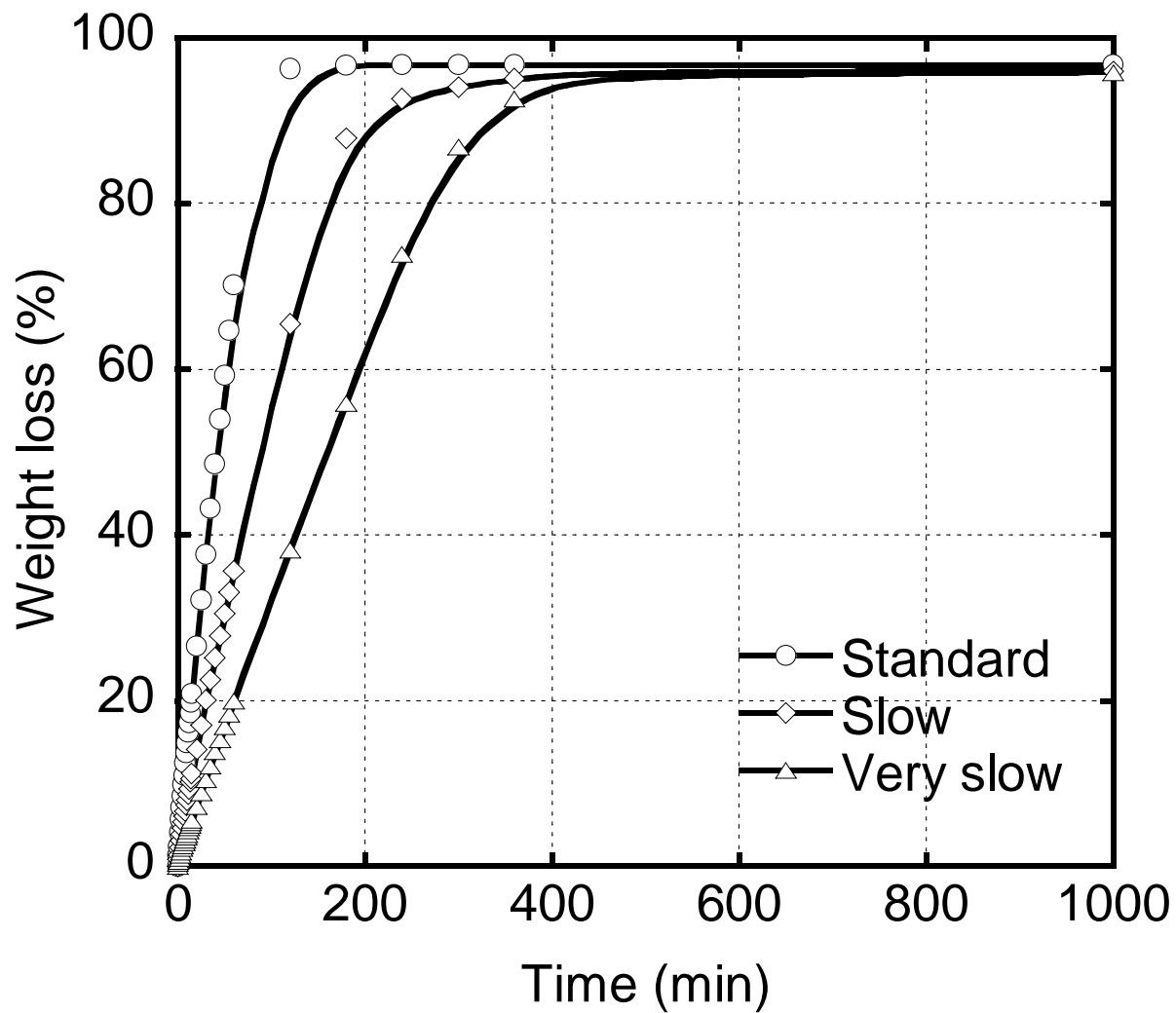
Songsurang et al., Figure 2



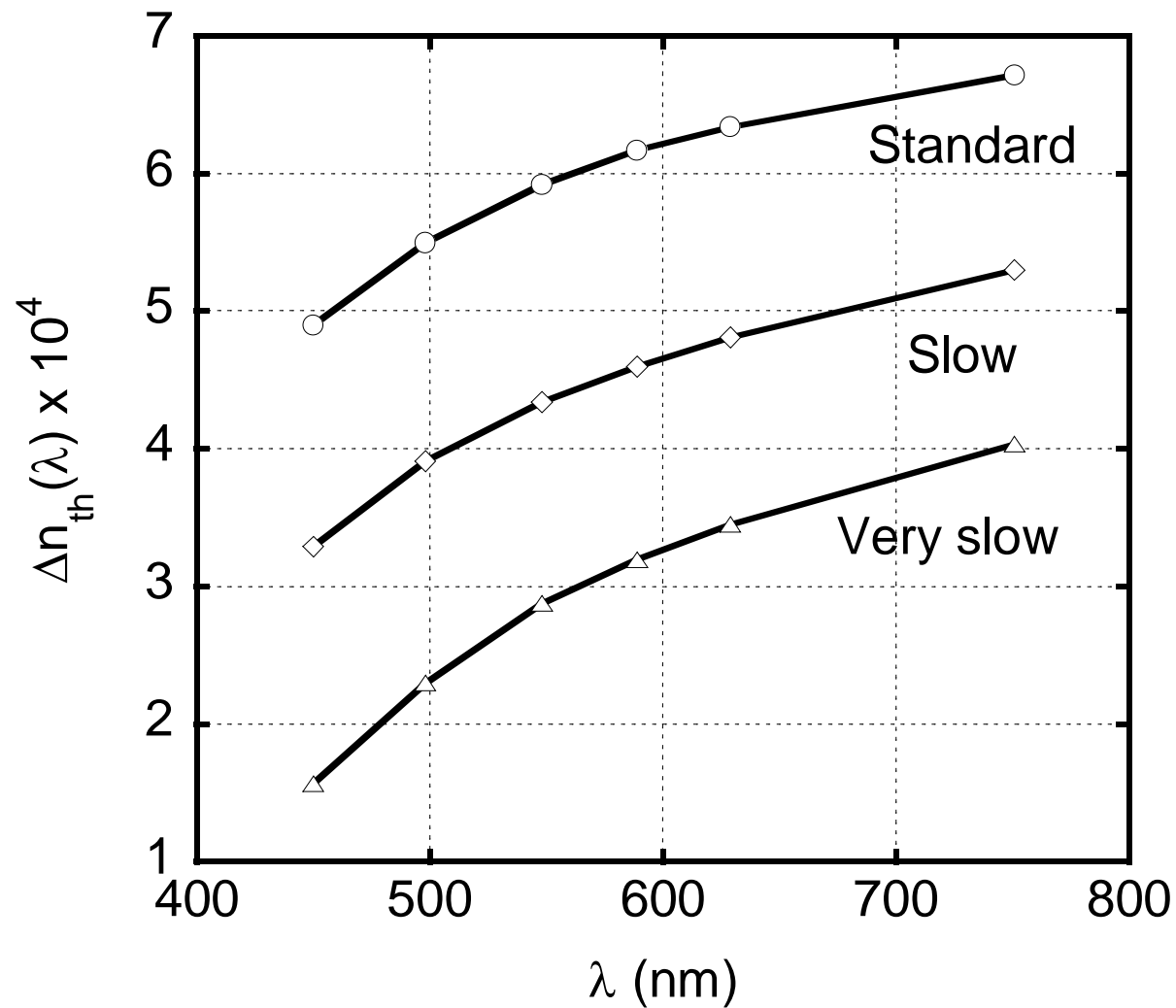
Songsurang et al., Figure 3



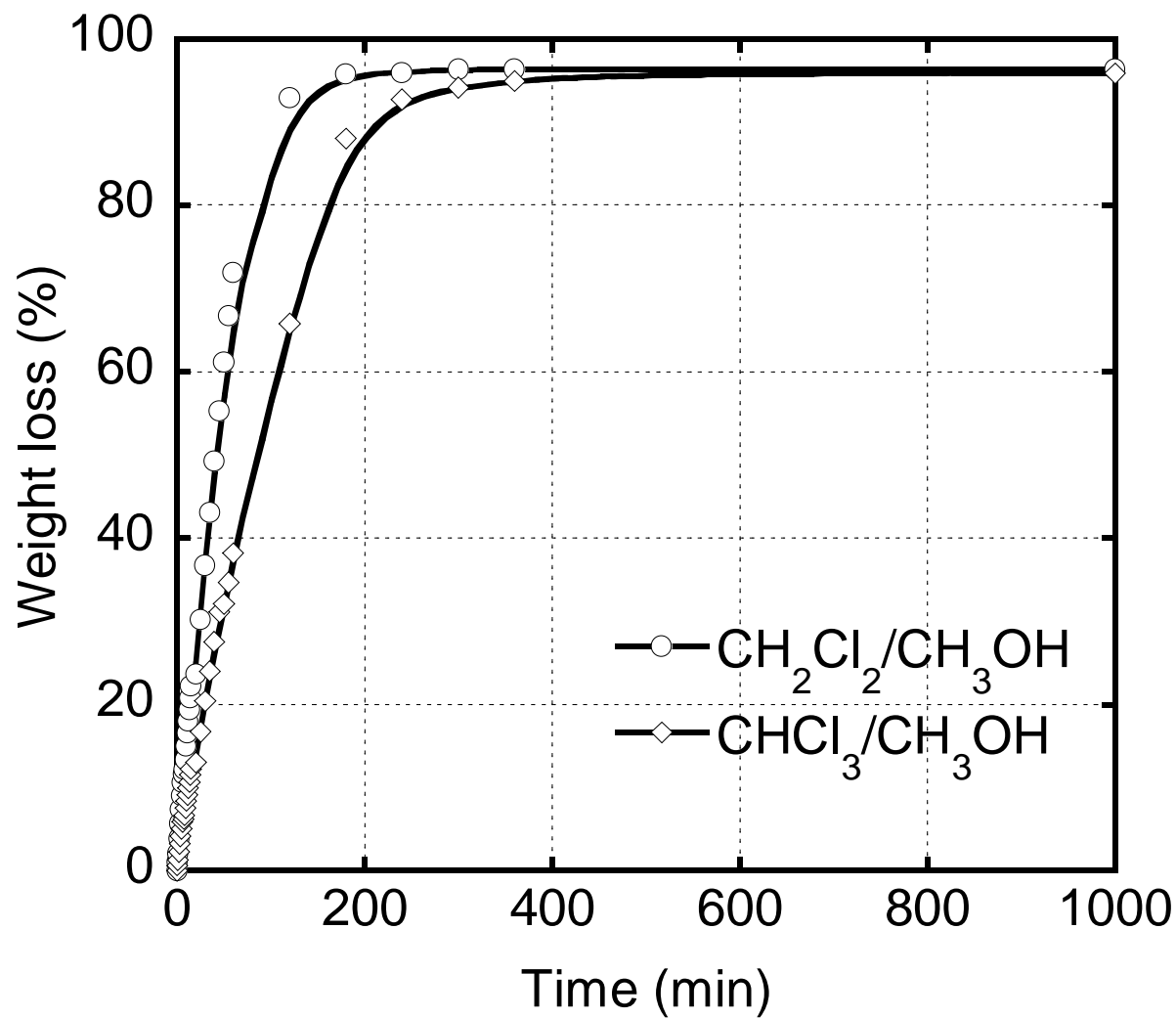
Songsurang et al., Figure 4



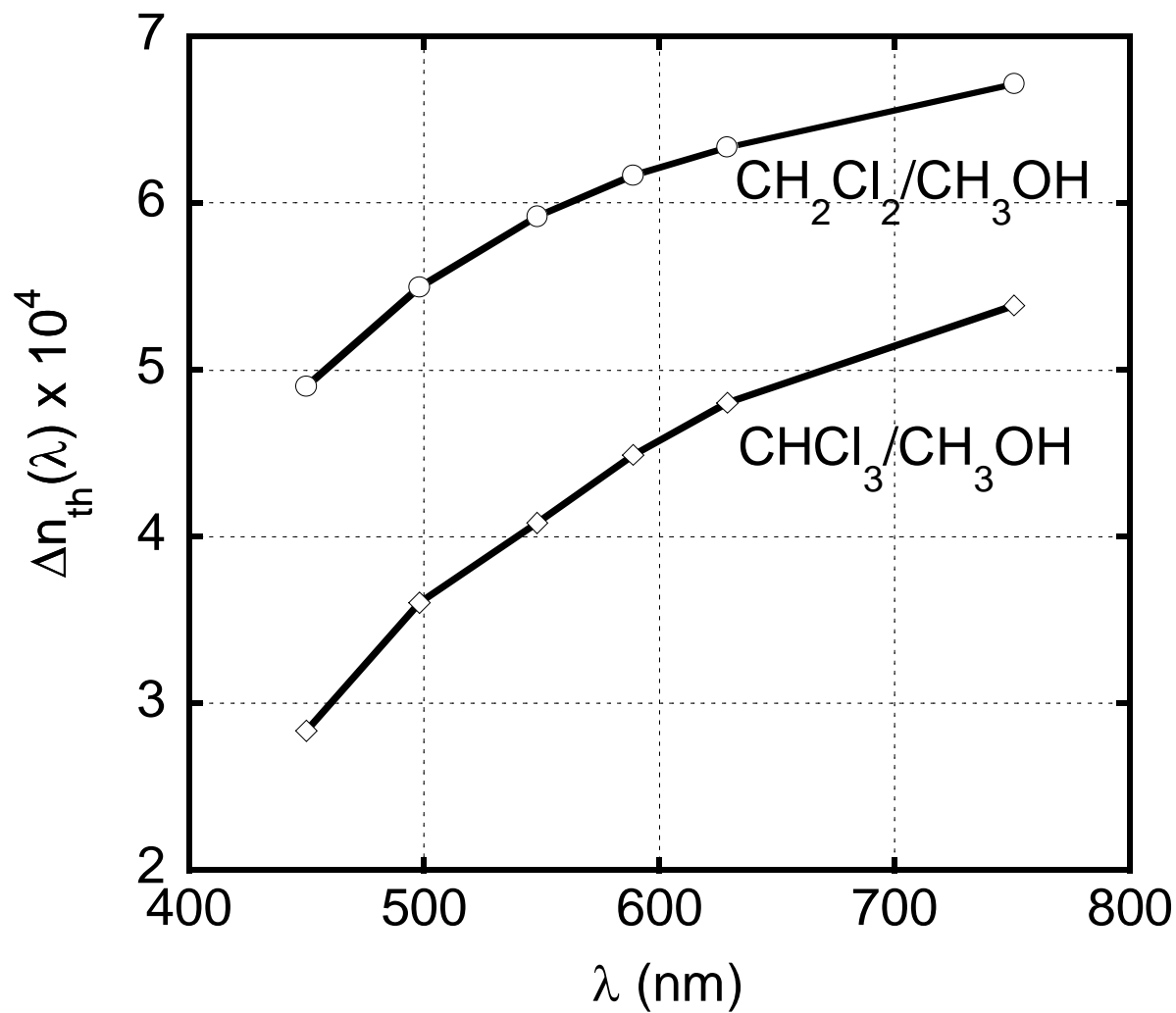
Songsurang et al., Figure 5



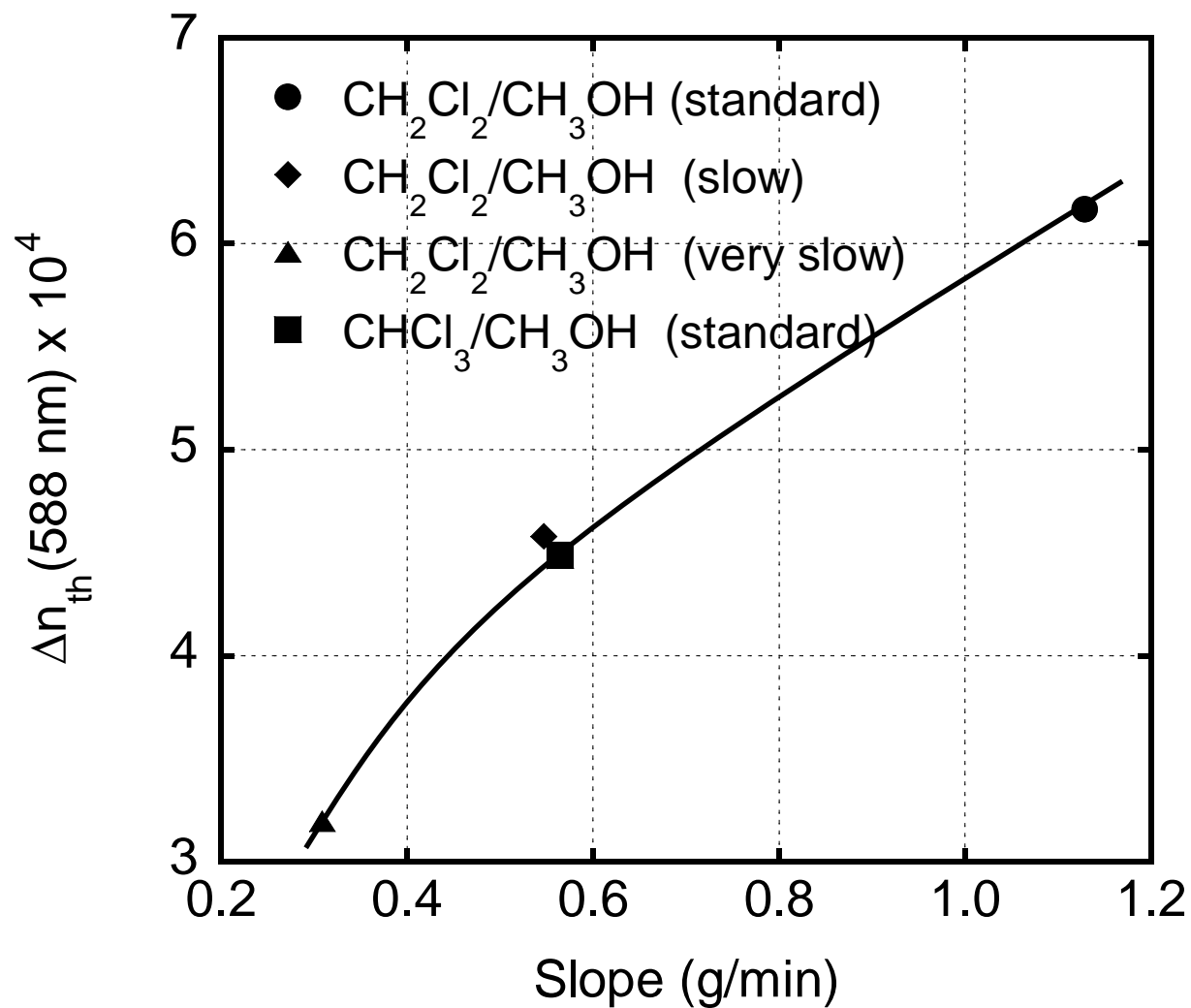
Songsurang et al., Figure 6



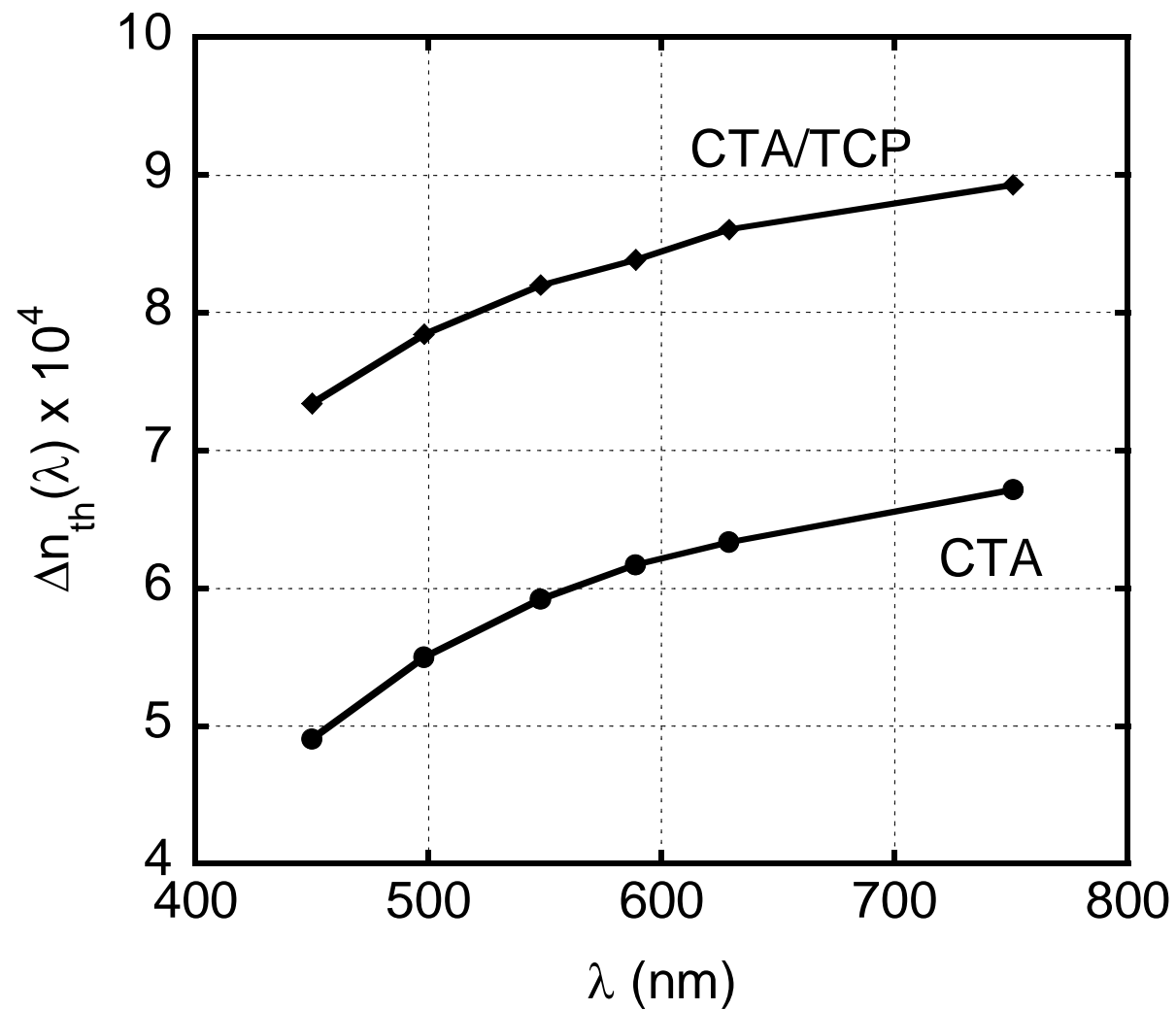
Songsurang et al., Figure 7



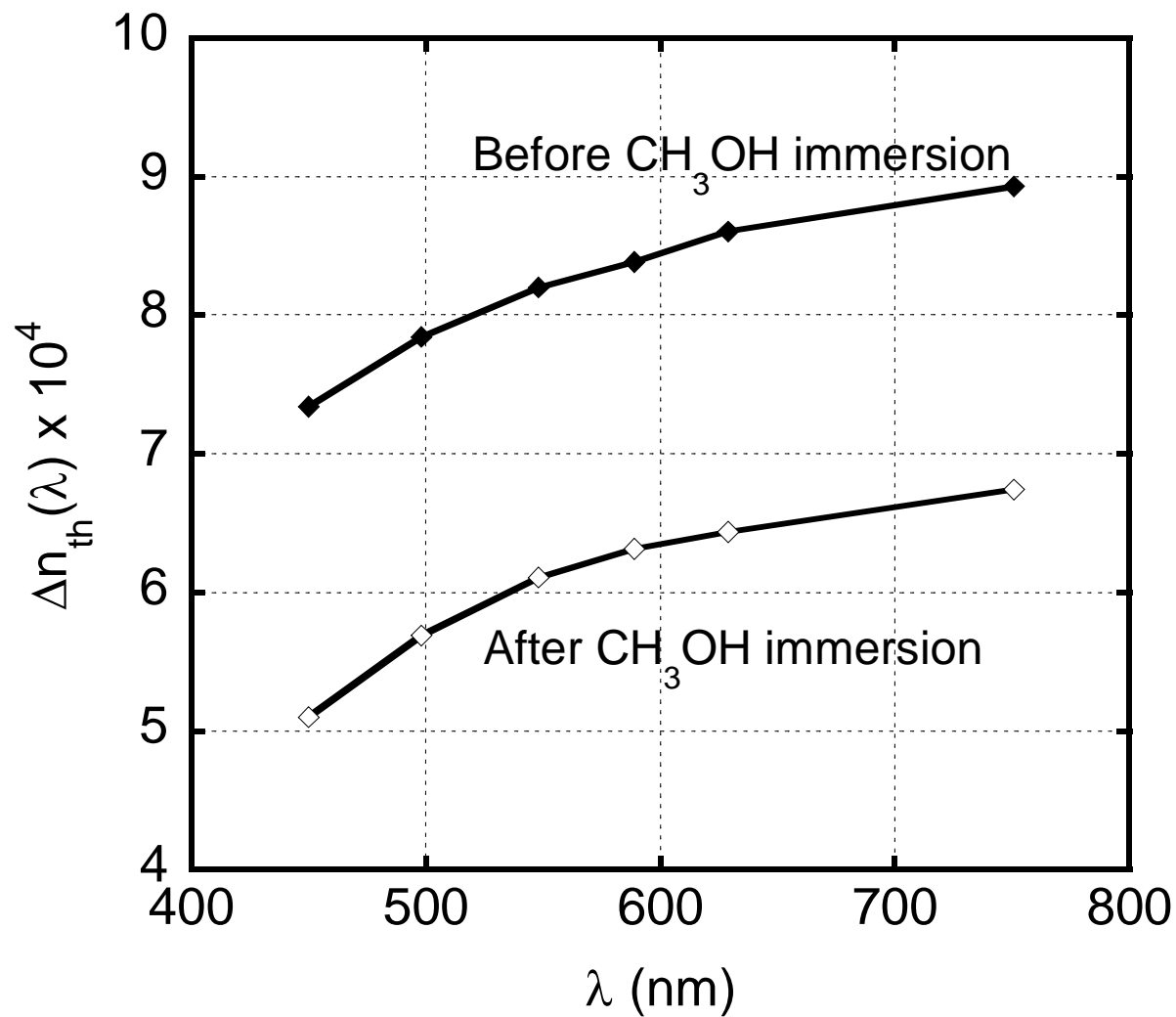
Songsurang et al., Figure 8



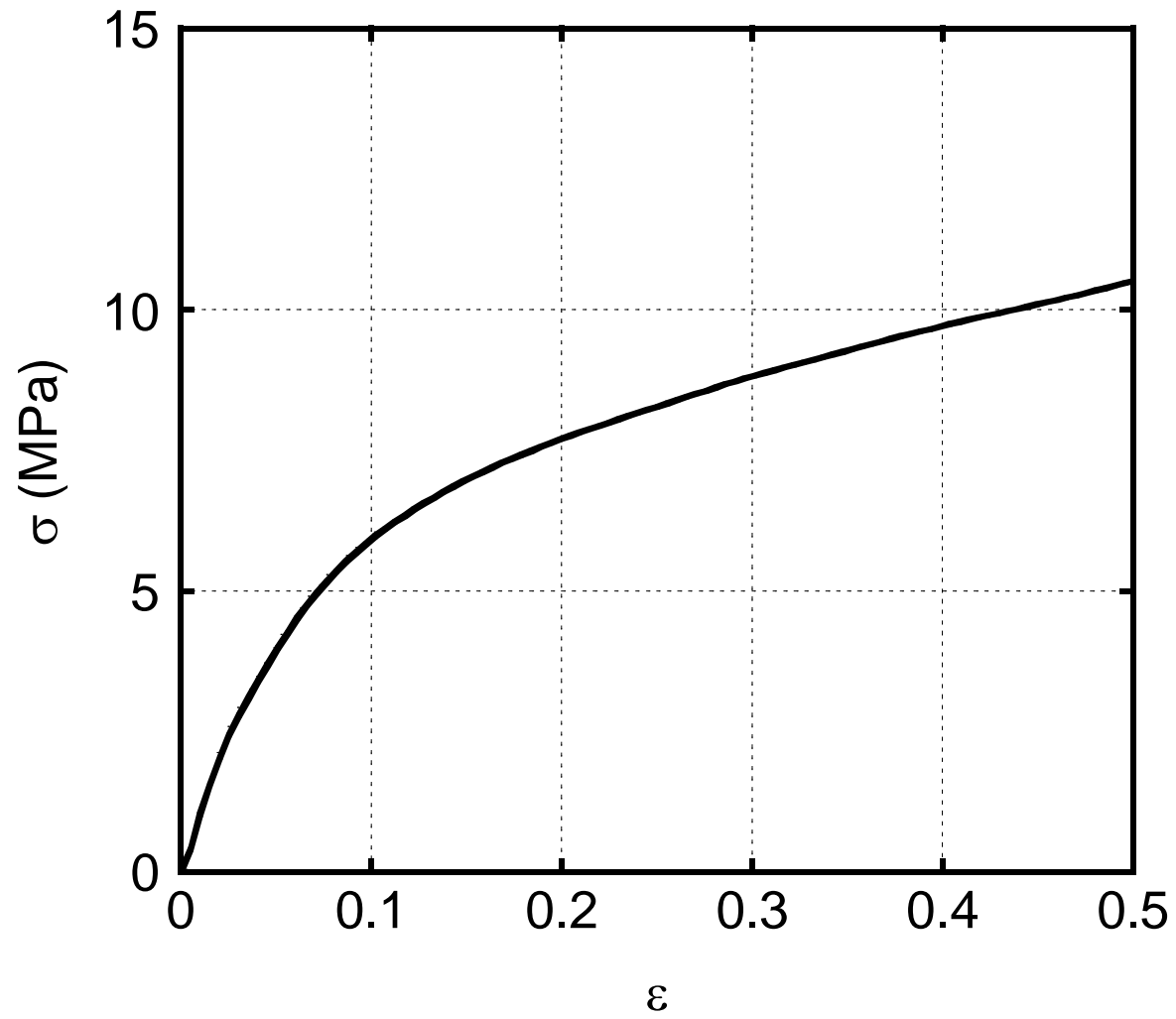
Songsurang et al., Figure 9



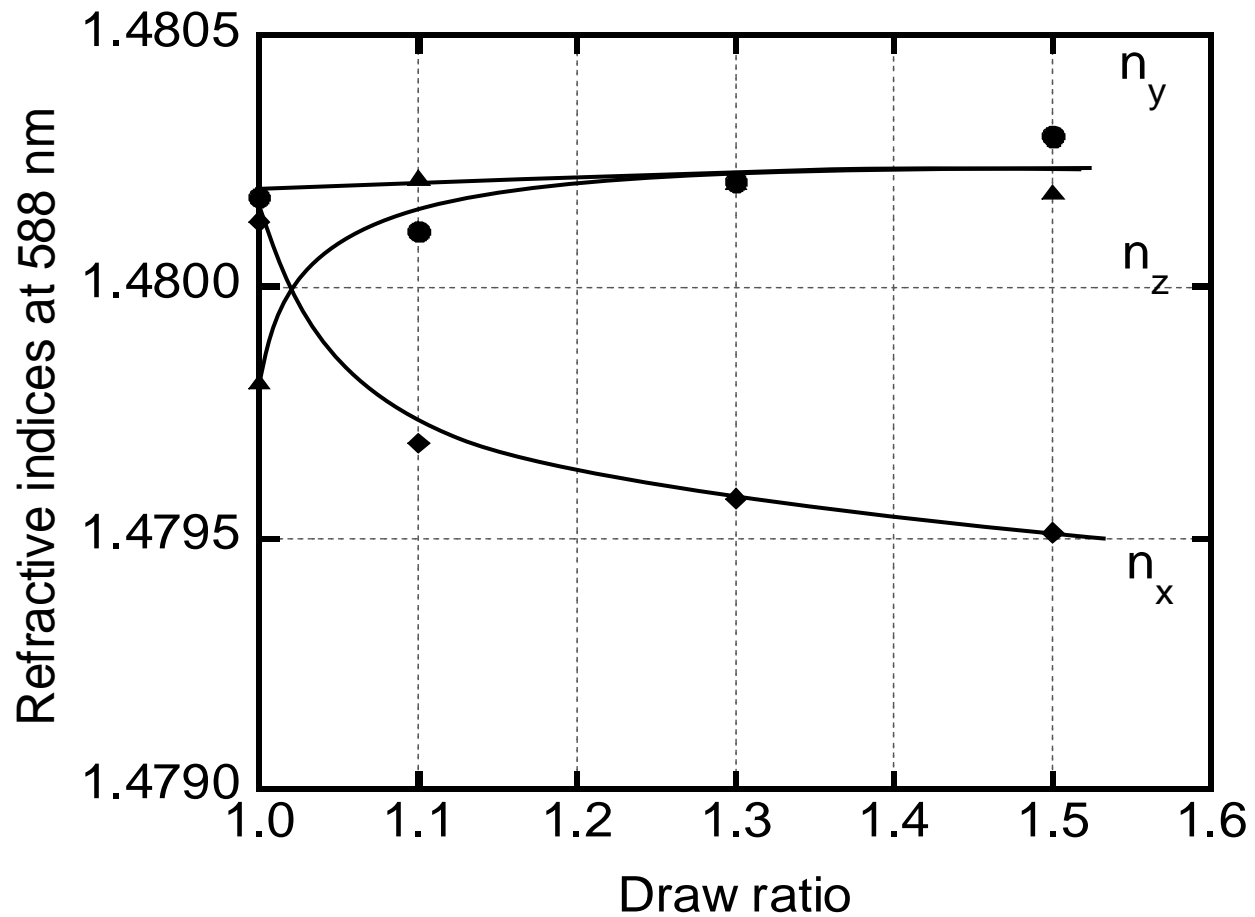
Songsurang et al., Figure 10



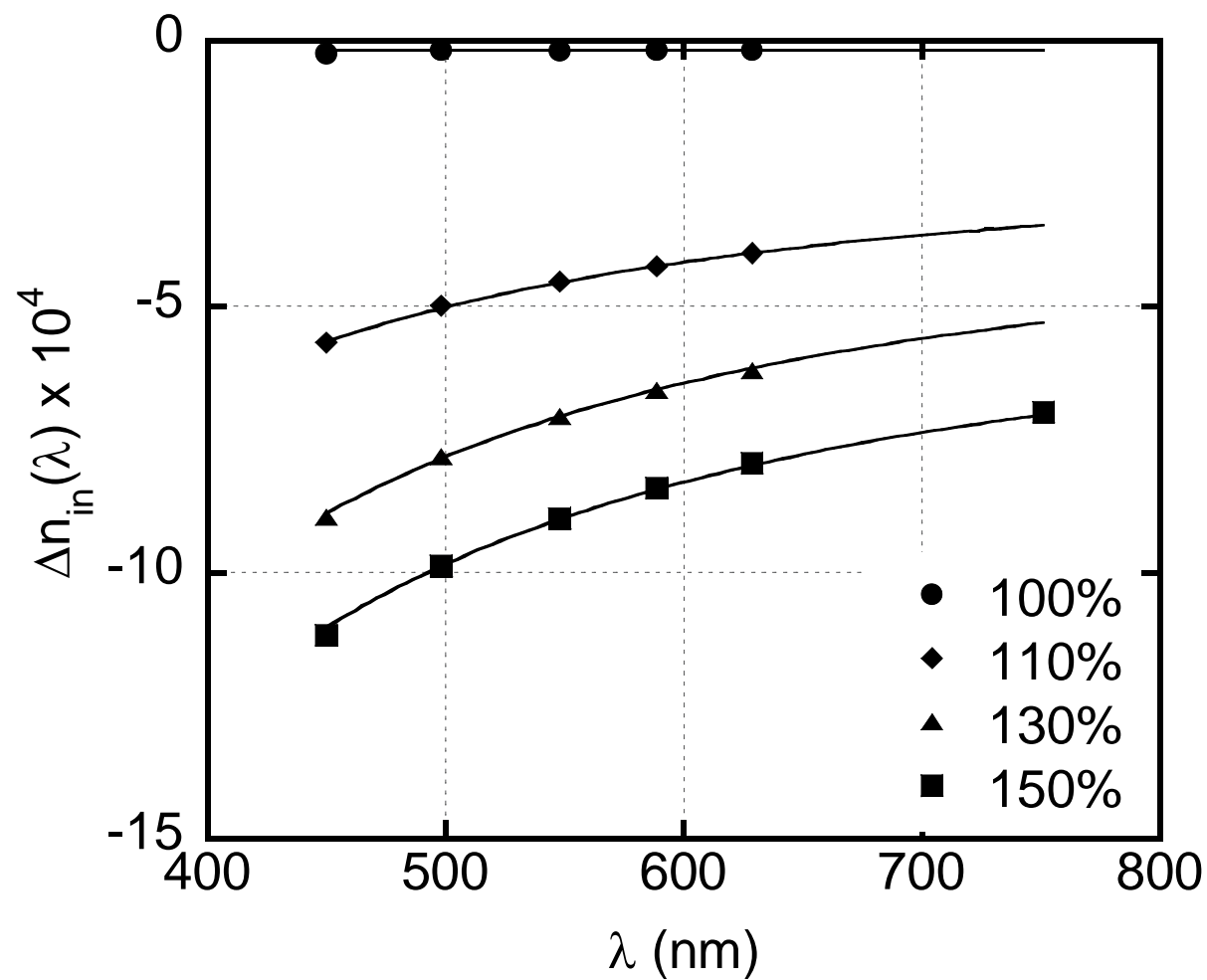
Songsurang et al., Figure 11



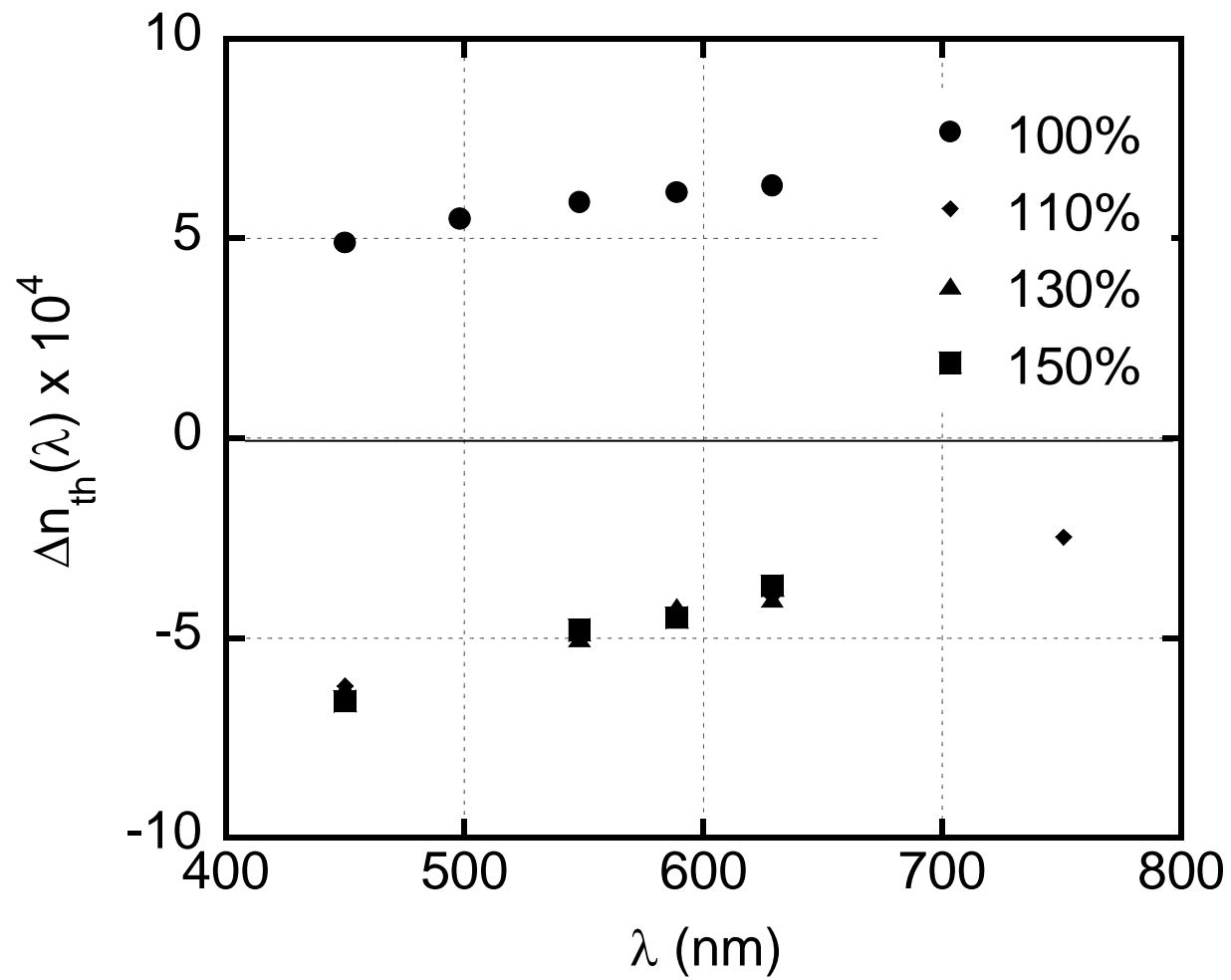
Songsurang et al., Figure 12



Songsurang et al., Figure 13



Songsurang et al., Figure 14a



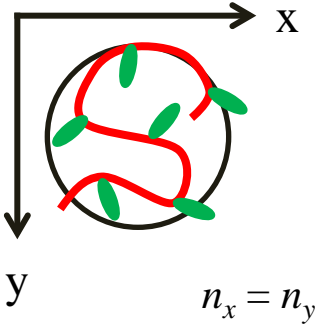
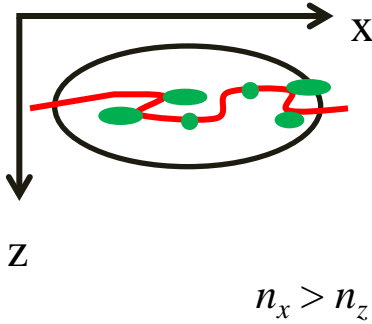
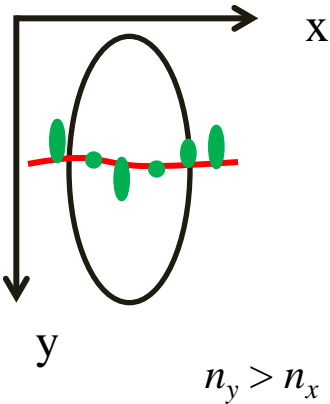
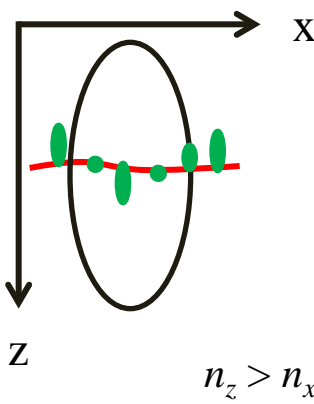
Songsurang et al., Figure 14b

Table 1. Thermal Properties of Solution-Cast Films Obtained by Various Conditions

Conditions				Heat of Fusion (J/g)
Thickness	Evaporation Rate	Solvent	TCP	
50 μm	Standard	$\text{CH}_2\text{Cl}_2/\text{CH}_3\text{OH}$	Not included	13.8
100 μm	Standard	$\text{CH}_2\text{Cl}_2/\text{CH}_3\text{OH}$	Not included	12.7
200 μm	Standard	$\text{CH}_2\text{Cl}_2/\text{CH}_3\text{OH}$	Not included	11.5
300 μm	Standard	$\text{CH}_2\text{Cl}_2/\text{CH}_3\text{OH}$	Not included	10.9
100 μm	Slow	$\text{CH}_2\text{Cl}_2/\text{CH}_3\text{OH}$	Not included	12.1
100 μm	Very slow	$\text{CH}_2\text{Cl}_2/\text{CH}_3\text{OH}$	Not included	11.3
100 μm	Standard	$\text{CHCl}_3/\text{CH}_3\text{OH}$	Not included	12.1
100 μm	Standard	$\text{CH}_2\text{Cl}_2/\text{CH}_3\text{OH}$	Included	10.2

Illustrations

Orientation of CTA molecules and refractive index ellipsoids of acetyl group

Film	Top-View	Side-View	Orientation of acetyl group & birefringence
<ul style="list-style-type: none"> As Cast <p>Polymer chains exist in the x-y plane.</p>	 <p>$n_x = n_y$</p>	 <p>$n_x > n_z$</p>	<p>perpendicular to the z direction.</p> <p>↓</p> <p>positive Δn_{th}</p>
<ul style="list-style-type: none"> After Stretching <p>Polymer chains are oriented in the x direction.</p>	 <p>$n_y > n_x$</p>	 <p>$n_z > n_x$</p>	<p>perpendicular to the x direction.</p> <p>↓</p> <p>negative Δn_{in}</p>